

碩士學位論文

Synthesis and Characterization of
Ni(II)–Oxaazamacrocyclic Complexes
Containing Auxiliary Ligands



Department of Chemistry
Graduate School
Cheju National University

Ki–Ju Kim

December, 2005


보조 리간드들을 포함하는 Ni(II)-Oxaaza 거대고리 착물들의 합성 및 물성 연구

지도교수 변 중 철

김 기 주

이 논문을 이학 석사학위 논문으로 제출함

2005년 12월

 제주대학교 중앙도서관
김기주의 이학 석사학위 논문을 인준함

심사위원장 _____인

위 원 _____인

위 원 _____인

제주대학교 대학원

2005년 12월

Synthesis and Characterization of
Ni(II)–Oxaazamacrocyclic Complexes
Containing Auxiliary Ligands

Ki–Ju Kim

(Supervised by professor Jong–Chul Byun)



A THESIS SUBMITTED IN PARTIAL FULFILLMENT OF THE
REQUIREMENTS FOR THE DEGREE OF MASTER OF
NATURAL SCIENCE

2005. 12.

DEPARTMENT OF CHEMISTRY
GRADUATE SCHOOL
CHEJU NATIONAL UNIVERSITY

Contents

List of Tables	ii
List of Figures	iv
Abstract	vi
I. Introduction	1
II. Experimental section	3
1. Physical Measurements	3
2. Synthesis of Ligand and Complexes	4
1) Preparation of 2,6-diformyl- <i>p</i> -cresol	4
2) Preparation of dinuclear Ni(II) complexes	4
3) Preparation of mononuclear Ni(II) complexes	8
3. X-ray Diffraction Measurements	11
III. Results and Discussion	21
1. IR spectra of the complexes	21
2. FAB-mass spectra of the complexes	35
3. Electronic absorption spectrum	46
4. Crystal Structures of Complexes	56
IV. Conclusion	68
References	72
Abstract(Korean)	

List of Tables

Table 1. Crystal data and structure refinement for $\text{Ni}_2([\text{20}]\text{-DCHDC})(\text{ClO}_4)_2 \cdot 2\text{CH}_3\text{CN}$ complex	12
Table 2. Atomic coordinates ($\times 10^4$) and equivalent isotropic displacement parameters ($\text{\AA}^2 \times 10^3$) for $[\text{Ni}_2([\text{20}]\text{-DCHDC})(\text{ClO}_4)_2 \cdot 2\text{CH}_3\text{CN}$ complex	13
Table 3. Anisotropic displacement parameters ($\text{\AA}^2 \times 10^3$) for $[\text{Ni}_2([\text{20}]\text{-DCHDC})(\text{ClO}_4)_2 \cdot 2\text{CH}_3\text{CN}$ complex	14
Table 4. Hydrogen coordinates ($\times 10^4$) and isotropic displacement parameters ($\text{\AA}^2 \times 10^3$) for $[\text{Ni}_2([\text{20}]\text{-DCHDC})(\text{ClO}_4)_2 \cdot 2\text{CH}_3\text{CN}$ complex	15
Table 5. Crystal data and structure refinement for $[\text{Ni}(\text{H}_2[\text{20}]\text{-DCHDC})(\text{ClO}_4)_2$ complex	17
Table 6. Atomic coordinates ($\times 10^4$) and equivalent isotropic displacement parameters ($\text{\AA}^2 \times 10^3$) for $[\text{Ni}(\text{H}_2[\text{20}]\text{-DCHDC})] \cdot 2\text{ClO}_4$ complex	18
Table 7. Anisotropic displacement parameters ($\text{\AA}^2 \times 10^3$) for $[\text{Ni}(\text{H}_2[\text{20}]\text{-DCHDC})] \cdot 2\text{ClO}_4$ complex	19
Table 8. Hydrogen coordinates ($\times 10^4$) and isotropic displacement parameters ($\text{\AA}^2 \times 10^3$) for $[\text{Ni}(\text{H}_2[\text{20}]\text{-DCHDC})] \cdot 2\text{ClO}_4$ complex	20
Table 9. Characteristic IR absorptions (cm^{-1}) of macrocyclic ligand ($\text{H}_2[\text{20}]\text{-DCHDC}$) for the Ni(II) complexes	24
Table 10. Characteristic IR absorptions (cm^{-1}) of exocyclic molecules for the Ni(II) complexes	26
Table 11. FAB-mass spectra for the binuclear Ni(II) complexes of phenol-based macrocyclic ligand ($\text{H}_2[\text{20}]\text{-DCHDC}$)	37

Table 12. Electronic spectral data (λ_{max} ; nm, ϵ ; $\text{M}^{-1} \text{cm}^{-1}$) for the Ni(II) macrocyclic complexes	47
Table 13. Bond lengths (\AA) for $[\text{Ni}_2([\text{20}]\text{-DCHDC})](\text{ClO}_4)_2 \cdot 2\text{CH}_3\text{CN}$ complex	60
Table 14. Angles [$^\circ$] for $[\text{Ni}_2([\text{20}]\text{-DCHDC})](\text{ClO}_4)_2 \cdot 2\text{CH}_3\text{CN}$ complex	61
Table 15. Bond lengths (\AA) for $[\text{Ni}(\text{H}_2[\text{20}]\text{-DCHDC})](\text{ClO}_4)_2$ complex	66
Table 16. Angles [$^\circ$] for $[\text{Ni}(\text{H}_2[\text{20}]\text{-DCHDC})](\text{ClO}_4)_2$ complex	67



List of Figures

Figure 1. FT-IR spectrum of $[\text{Ni}_2([\text{20}]\text{-DCHDC})]\text{Cl}_2$ complex	27
Figure 2. FT-IR spectrum of $[\text{Ni}_2([\text{20}]\text{-DCHDC})](\text{ClO}_4)_2$ complex	28
Figure 3. FT-IR spectrum of $[\text{Ni}_2([\text{20}]\text{-DCHDC})(\text{NCS})_2]$ complex	29
Figure 4. FT-IR spectrum of $[\text{Ni}_2([\text{20}]\text{-DCHDC})(\text{N}_3)_2]$ complex	30
Figure 5. FT-IR spectrum of $[\text{Ni}_2([\text{20}]\text{-DCHDC})(\mu\text{-ONO})]\text{NO}_2 \cdot 1.5\text{H}_2\text{O}$ complex	31
Figure 6. FT-IR spectrum of $[\text{Ni}_2([\text{20}]\text{-DCHDC})\text{I}_2]$ complex.	32
Figure 7. FT-IR spectrum of $[\text{Ni}(\text{H}_2[\text{20}]\text{-DCHDC})](\text{ClO}_4)_2 \cdot 2\text{H}_2\text{O}$ complex	33
Figure 8. FT-IR spectrum of $[\text{Ni}(\text{H}_2[\text{20}]\text{-DCHDC})(\text{NCS})_2] \cdot 3\text{H}_2\text{O}$ complex	34
Figure 9. FAB mass spectrum of the $[\text{Ni}_2([\text{20}]\text{-DCHDC})]\text{Cl}_2$	38
Figure 10. FAB mass spectrum of the $[\text{Ni}_2([\text{20}]\text{-DCHDC})](\text{ClO}_4)_2$	39
Figure 11. FAB mass spectrum of the $[\text{Ni}_2([\text{20}]\text{-DCHDC})(\text{NCS})_2]$	40
Figure 12. FAB mass spectrum of the $[\text{Ni}_2([\text{20}]\text{-DCHDC})(\text{N}_3)_2]$	41
Figure 13. FAB mass spectrum of the $[\text{Ni}_2([\text{20}]\text{-DCHDC})(\mu\text{-ONO})]\text{NO}_2 \cdot 1.5\text{H}_2\text{O}$	42
Figure 14. FAB mass spectrum of the $[\text{Ni}_2([\text{20}]\text{-DCHDC})(\text{I})_2]$	43
Figure 15. FAB mass spectrum of the $[\text{Ni}(\text{H}_2[\text{20}]\text{-DCHDC})](\text{ClO}_4)_2 \cdot 2\text{H}_2\text{O}$	44
Figure 16. FAB mass spectrum of the $[\text{Ni}(\text{H}_2[\text{20}]\text{-DCHDC})(\text{NCS})_2] \cdot 3\text{H}_2\text{O}$	45
Figure 17. Electronic absorption spectrum of $[\text{Ni}_2([\text{20}]\text{-DCHDC})]\text{Cl}_2$ in (a) methanol ($1.0 \times 10^{-4}\text{M}$) and (b) solid (BaSO_4)	48
Figure 18. Electronic absorption spectrum of $[\text{Ni}_2([\text{20}]\text{-DCHDC})](\text{ClO}_4)_2$ in (a) DMSO ($1.0 \times 10^{-4}\text{M}$) and (b) solid (BaSO_4)	49

Figure 19. Electronic absorption spectrum of $[\text{Ni}_2([\text{20}]\text{-DCHDC})(\text{NCS})_2]$ in (a) DMSO ($1.0 \times 10^{-4} \text{M}$) and (b) solid (BaSO_4)	50
Figure 20. Electronic absorption spectrum of $[\text{Ni}_2([\text{20}]\text{-DCHDC})(\text{N}_3)_2]$ in (a) DMSO ($1.0 \times 10^{-4} \text{M}$) and (b) solid (BaSO_4)	51
Figure 21. Electronic absorption spectrum of $[\text{Ni}_2([\text{20}]\text{-DCHDC})(\mu\text{-ONO})]\text{NO}_2 \cdot 1.5\text{H}_2\text{O}$ in (a) DMSO ($1.0 \times 10^{-4} \text{M}$) and (b) solid (BaSO_4)	52
Figure 22. Electronic absorption spectrum of $[\text{Ni}_2([\text{20}]\text{-DCHDC})(\text{I})_2]$ in (a) DMSO ($1.0 \times 10^{-4} \text{M}$) and (b) solid (BaSO_4)	53
Figure 23. Electronic absorption spectrum of $[\text{Ni}(\text{H}_2[\text{20}]\text{-DCHDC})](\text{ClO}_4)_2 \cdot 2\text{H}_2\text{O}$ in (a) DMSO ($1.0 \times 10^{-4} \text{M}$) and (b) solid (BaSO_4)	54
Figure 24. Electronic absorption spectrum of $[\text{Ni}(\text{H}_2[\text{20}]\text{-DCHDC})(\text{NCS})_2] \cdot 3\text{H}_2\text{O}$ in (a) DMSO ($1.0 \times 10^{-4} \text{M}$) and (b) solid (BaSO_4)	55
Figure 25. Structural representation of asymmetric unit of $[\text{Ni}_2([\text{20}]\text{-DCHDC})](\text{ClO}_4)_2 \cdot 2\text{CH}_3\text{CN}$ complex	56
Figure 26. An ORTEP view of core structure (top view) for the binuclear complex showing 50% probability thermal ellipsoids and labels for non-H atoms	57
Figure 27. The molecular packing diagram of $[\text{Ni}_2([\text{20}]\text{-DCHDC})](\text{ClO}_4)_2 \cdot 2\text{CH}_3\text{CN}$	59
Figure 28. Structural representation of asymmetric unit of $[\text{Ni}(\text{H}_2[\text{20}]\text{-DCHDC})](\text{ClO}_4)_2$ complex	62
Figure 29. An ORTEP view of core structure (top view) for the mononuclear complex showing 50% probability thermal ellipsoids and labels for non-H atoms.	63
Figure 30. The molecular packing diagram of $[\text{Ni}(\text{H}_2[\text{20}]\text{-DCHDC})](\text{ClO}_4)_2$	65

Abstract

Binuclear Ni(II) complex $\{[\text{Ni}_2([\text{20}]\text{-DCHDC})\text{Cl}_2]\}$, with $[2 + 2]$ symmetrical N_4O_2 compartmental macrocyclic ligand $\{\text{H}_2[\text{20}]\text{-DCHDC}; 14,29\text{-dimethyl-3,10,18,25-tetraazapentacyclo-[25,3,1,0}^{4,9},1^{12,16},0^{19,24}]\text{ditriacontane-2,10,12,14,16(32),17,27(31),28,30-decane-31,32-diol}\}$ containing bridging phenolic oxygen atoms was synthesized by metal template condensation of 2,6-diformyl-*p*-cresol, *trans*-1,2-diaminocyclohexane and nickel chloride hexahydrate. The reaction of $[\text{Ni}_2([\text{20}]\text{-DCHDC})\text{Cl}_2$ with auxiliary ligands (L_a ; ClO_4^- , SCN^- , N_3^- , NO_2^- , and I^-) in methanol solution formed a new 5 complexes; $[\text{Ni}_2([\text{20}]\text{-DCHDC})\text{-(ClO}_4)_2$, $[\text{Ni}_2([\text{20}]\text{-DCHDC})(\text{NCS})_2]$, $[\text{Ni}_2([\text{20}]\text{-DCHDC})(\text{N}_3)_2]$, $[\text{Ni}_2([\text{20}]\text{-DCHDC})\text{-(}\mu\text{-ONO)}\text{]NO}_2 \cdot 1.5\text{H}_2\text{O}$, and $[\text{Ni}_2([\text{20}]\text{-DCHDC})\text{I}_2]$. Mononuclear Ni(II) complex $([\text{Ni}(\text{H}_2[\text{20}]\text{-DCHDC})](\text{ClO}_4)_2 \cdot 2\text{H}_2\text{O})$, with $[2+2]$ symmetrical N_4O_2 compartmental macrocyclic ligand containing bridging phenolic oxygen atoms was synthesized by metal template condensation of 2,6-diformyl-*p*-cresol, *trans*-1,2-diaminocyclohexane and nickel perchlorate hexahydrate. The reaction of $([\text{Ni}(\text{H}_2[\text{20}]\text{-DCHDC})](\text{ClO}_4)_2 \cdot 2\text{H}_2\text{O}$ with auxiliary ligand (L_a ; SCN^-) in methanol solution formed $([\text{Ni}([\text{22}]\text{-DCHDC})(\text{NCS})_2] \cdot 3\text{H}_2\text{O})$. X-ray crystals and molecular structures of $([\text{Ni}_2([\text{20}]\text{-DCHDC})](\text{ClO}_4)_2 \cdot 2\text{CH}_3\text{CN})$ and $([\text{Ni}(\text{H}_2[\text{20}]\text{-DCHDC})](\text{ClO}_4)_2)$ have been determined on a XRD. The binuclear $([\text{Ni}_2([\text{20}]\text{-DCHDC})](\text{ClO}_4)_2 \cdot 2\text{CH}_3\text{CN})$ core structures are centrosymmetric with each nickel(II) ion in the N_2O_2 sites being four-coordinate by square-planar geometry of interactions with two nitrogen and two oxygen atoms of the binucleating ligand $[\text{20}]\text{-DCHDC}$. $([\text{Ni}_2([\text{20}]\text{-DCHDC})](\text{ClO}_4)_2)$ has two uncoordinated perchlorate anions, two acetonitrile molecule in the crystal lattice. The Ni-N(3) (acetonitrile) and Ni-O(16) (perchlorate) separation are 3.256 and 4.759 Å, respectively. The interatomic Ni \cdots Ni separation is 2.8078(10) Å.

the $[\text{Ni}(\text{H}_2[20]\text{-DCHDC})](\text{ClO}_4)_2$ crystals, the occupancy of central metal Ni(II) is 0.5 in two N_2O_2 sites. The geometry about Ni(1) in the N_2O_2 site is a square-planar environment, and other N_2O_2 site is able to vacant. The macrocyclic complex adopts an essentially flat structure with the square-planar nickel center bridged by the two phenoxide oxygen atoms. The sum of angles at the nickel basal planes (NiN_2O_2) is almost exactly 360° , indicating no plane distortion. Two phenol mean planes are not able to flat. The in-plane Ni-to-donor distances range from 1.743(4) to 1.907(6) Å. The perchlorate ions occupy lattice sites. The Ni(1)⋯O(2) (perchlorate) separation is 3.453(6) Å.



I. Introduction

Interest in exploring metal ion complexes with macrocyclic ligands has been continually increasing owing to the recognition of their role played by these structures in metalloproteins. Schiff base macrocycles have been of great importance in macrocyclic chemistry. They were among the first artificial metal macrocyclic complexes to be synthesized. The metal complexes containing synthetic macrocyclic ligands have attracted a great deal of attention because they can be used as models for more intricate biological macrocyclic systems: metalloporphyrins (hemoglobin, myoglobin, cytochrome, chlorophyll), corrins (vitamin B₁₂) and antibiotics (valinomycin, nonactin). These discoveries have created supramolecular chemistry and its enormous diversity.¹⁻⁵

Over the past decade, many studies have been focused upon metal complexes of cyclic triamines which cleaving carboxyester,⁶ phos-phoeaster,⁷⁻¹¹ RNA,^{12,13} DNA,^{14,15} dipeptides and proteins.¹⁶ To our knowledge, few papers published for the cytotoxic properties and the *in vivo* antitumor effects of triazacyclic polyamines metal complexes.^{17,18}

Ni(II) complexes with polyamine ligands containing binding units suited for the coordination of a single metal ion or for the dinuclear centers have proved very useful. The structure of these synthetic dioxygen carriers, the kinetics and thermo-dynamics of their formation is affected by the nature of the ligand. The use of polynucleating ligands represents an evolution in synthetic Ni(II) dioxygen carriers. These ligands contain sufficient number of oxygen and nitrogen donor atoms to coordinate more than one Ni(II) ion and can act as biomimetic models of natural non-heme types carriers, such as hemerythrin and hemocyanin.¹⁹

The Schiff base macrocyclic complexes, which form neutral or cationic

complexes with the metal of interest, fulfill these requirements, because they are extremely rigid and display kinetic inertness towards metal release, whereas exocyclic ligands are labile and easy to change.

Macrocyclic Schiff bases have been widely studied because they can selectively chelate certain metal ions depending on the number, type and position of their donor atoms, the ionic radius of the metal center, and coordinating properties of counter ions.²⁰

This work performs synthesis, crystal X-ray diffraction studies and physicochemical characterization of dinuclear Ni(II) and mononuclear Ni(II) complexes, with [2+2] symmetrical N₄O₂ compartmental macrocyclic ligand {H₂[20]-DCHDC;14,29-dimethyl-3,10,18,25-tetraazapentacyclo-[25,3,1,0^{4,9},1^{12,16},0^{19,24}]ditriacontane-2,10,12,14,16(32),17,27(31),28,30-decane-31,32-diol} containing bridging phenolic oxygen atoms was synthesized by condensation, in the metal ions, of 2,6-diformyl-*p*-cresol and *trans*-1,2-diaminocyclohexane.



II. Experimental section

1. Physical Measurements

All chemicals were commercial analytical reagents and were used without further purification. For the spectroscopic and physical measurements, organic solvents were dried and purified according to the literature methods. Nanopure quality water was used throughout this work. Microanalyses of C, H, and N were carried out using LECO CHN-900 analyzer. Conductance measurements of the complexes were performed at $25\pm 1^\circ\text{C}$ using an ORION 162 conductivity temperature meter. IR spectra were recorded with a Bruker FSS66 FT-IR spectrometer in the range $4000\text{-}370\text{ cm}^{-1}$ using KBr pellets. Electronic absorption spectra were measured at 25°C on a UV-3150 UV-VIS-NIR Spectrophotometer (SHIMADZU). FAB-mass spectra were obtained on a JEOL JMS-700 Mass Spectrometer using argon (6 kV, 10 mA) as the FAB gas. The accelerating voltage was 10 kV and glycerol or *m*-nitrobenzyl alcohol (NBA) was used as the matrix. The mass spectrometer was operated in positive ion mode and mass spectrum was calibrated by Alkali-CsI positive.

2. Synthesis of Ni(II) Complexes

1) Preparation of 2, 6-diformyl-*p*-cresol

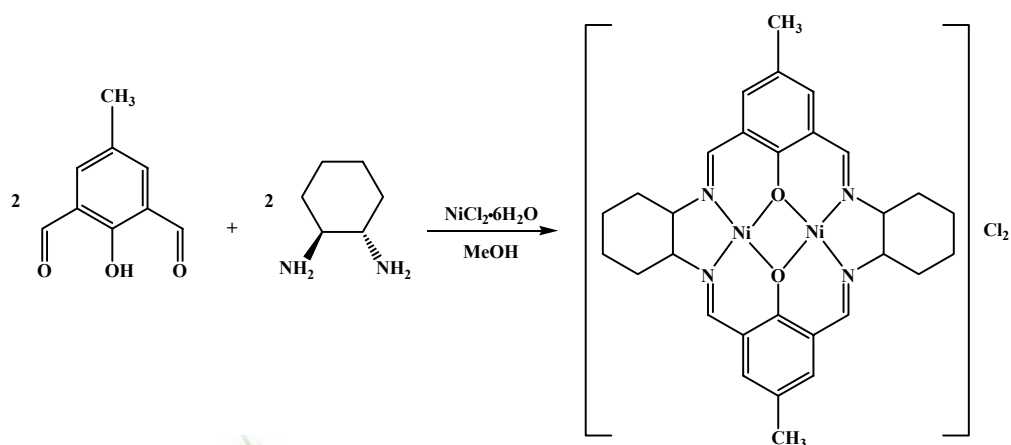
The synthesis of 2,6-diformyl-*p*-cresol was prepared according to the methods previously reported.^{21,22}

2) Preparation of dinuclear Ni(II) complexes

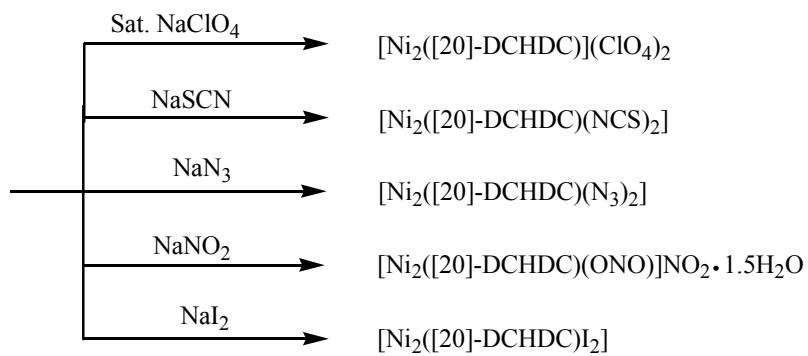
The dinuclear Ni(II) complexes with [2+2] symmetrical N₄O₂ compartmental macrocyclic ligand {[20]-DCHDC}²⁺ containing bridging phenolic oxygen atoms was synthesized by condensation of 2,6-diformyl-*p*-cresol and *trans*-1,2-diaminocyclohexane, in the Ni(II) ions (Scheme 1).

(1) [Ni₂([20]-DCHDC)]Cl₂

Nickel chloride hexahydrate (9.50 g), 2,6-diformyl-*p*-cresol (4.92 g), and *trans*-1,2-diaminocyclohexane (3.42 g) in methanol (200 mL) were refluxed for 1 day. The solution was concentrated under rota evaporation to approximate 50 mL and then it was on standing overnight at room temperature. The resulting dark brown precipitate was filtered, thoroughly washed twice with methanol, dried under vacuum over anhydrous calcium chloride.




 제주대학교 중앙도서관
 JEJU NATIONAL UNIVERSITY LIBRARY



Scheme 1. Synthesis of the dinuclear Ni(II) complexes of phenol-based macrocyclic ligand.

Yield : 4.4151 g (43.9%)

Anal. Calc.(%) for $\text{Ni}_2(\text{C}_{30}\text{H}_{34}\text{N}_4\text{O}_2)\text{Cl}_2$

C, 53.71 ; H, 5.11 ; N, 8.35

Found(%) C, 54.05 ; H, 5.01 ; N, 8.51

Solubility : MeOH, DMSO, DMF

λ_M (MeOH) : $169.3 \text{ ohm}^{-1}\text{cm}^2\text{mol}^{-1}$

(2) $[\text{Ni}_2([\text{20}]\text{-DCHDC})](\text{ClO}_4)_2$

A solution of $[\text{Ni}_2([\text{20}]\text{-DCHDC})]\text{Cl}_2$ (0.670 g) in methanol (150 mL) was added dropwise a saturated aqueous NaClO_4 solution (4 mL) with stirring and the mixture was refluxed for 6 h. The resulting orange precipitate were filtered, thoroughly washed twice with methanol, and dried under vacuum.

Yield : 0.5325 g (67.4%)

Anal. Calc.(%) for $\text{Ni}_2(\text{C}_{30}\text{H}_{34}\text{N}_4\text{O}_2)(\text{ClO}_4)_2$

C, 45.10 ; H, 4.29 ; N, 7.01

Found(%) C, 44.83 ; H, 4.30 ; N, 7.04

Solubility : Acetonitrile, DMSO, DMF

λ_M (MeOH) : $311 \text{ ohm}^{-1}\text{cm}^2\text{mol}^{-1}$

(3) $[\text{Ni}_2([\text{20}]\text{-DCHDC})(\text{NCS})_2]$

A solution of $[\text{Ni}_2([\text{20}]\text{-DCHDC})]\text{Cl}_2$ (0.670 g) in methanol (150 mL) was added dropwise of sodium thiocyanide (0.8107 g) with stirring and the mixture was refluxed for 6 h. The resulting dark brown precipitate were filtered, thoroughly washed twice with cold methanol, and dried under vacuum.

Yield : 0.6101 g (85.2%)

Anal. Calc.(%) for $\text{Ni}_2(\text{C}_{30}\text{H}_{34}\text{N}_4\text{O}_2)(\text{NCS})_2$

C, 53.67 ; H, 4.79 ; N, 11.73

Found(%) C, 54.53 ; H, 5.05 ; N, 11.86

Solubility : MeOH, DMSO, DMF

λ_M (DMSO) : 65.4 $\text{ohm}^{-1}\text{cm}^2\text{mol}^{-1}$

(4) $[\text{Ni}_2([\text{20}]\text{-DCHDC})(\text{N}_3)_2]$

A solution of $[\text{Ni}_2([\text{20}]\text{-DCHDC})]\text{Cl}_2$ (0.670 g) in methanol (150 mL) was added dropwise of sodium azide (0.6501 g) with stirring and the mixture was refluxed for 6 h. The resulting dark brown precipitate were filtered, thoroughly washed twice with cold methanol, and dried under vacuum.

Yield : 0.3826 g (55.9%)

Anal. Calc.(%) for $\text{Ni}_2(\text{C}_{30}\text{H}_{34}\text{N}_4\text{O}_2)(\text{N}_3)_2$

C, 52.68 ; H, 5.01 ; N, 20.48

Found(%) C, 52.23 ; H, 5.00 ; N, 19.91

Solubility : MeOH, DMSO

λ_M (DMSO) : 40.1 $\text{ohm}^{-1}\text{cm}^2\text{mol}^{-1}$

(5) $[\text{Ni}_2([\text{20}]\text{-DCHDC})(\mu\text{-ONO})]\text{NO}_2 \cdot 1.5\text{H}_2\text{O}$

A solution of $[\text{Ni}_2([\text{20}]\text{-DCHDC})]\text{Cl}_2$ (0.670 g) in methanol (150 mL) was added dropwise a solution of sodium nitrite (0.69 g) with stirring and the mixture was refluxed whereupon the initial red-brown precipitate first turned dark orange. The resulting dark brown precipitate were filtered, thoroughly washed twice with methanol, and dried under vacuum.

Yield : 0.3236 g (43.5%)

Anal. Calc.(%) for $\text{Ni}_2(\text{C}_{30}\text{H}_{34}\text{N}_4\text{O}_2)(\text{NO}_2)_2(\text{H}_2\text{O})_{1.5}$

C, 51.73 ; H, 5.02 ; N, 11.31

Found(%) C, 51.45 ; H, 4.94 ; N, 11.92

Solubility : MeOH

λ_M (MeOH) : $135.7 \text{ ohm}^{-1}\text{cm}^2\text{mol}^{-1}$

(6) $[\text{Ni}_2([\text{20}]\text{-DCHDC})\text{I}_2]$

A solution of $[\text{Ni}_2([\text{20}]\text{-DCHDC})]\text{Cl}_2$ (0.670 g) in methanol (150 mL) was added dropwise of sodium Iodine (1.4988 g) in methanol (50 mL) with stirring and the mixture was refluxed for 6 h. The resulting dark brown precipitate were filtered, thoroughly washed twice with cold methanol, and dried under vacuum.

Yield : 0.6325 g (74%)

Anal. Calc.(%) for $\text{Ni}_2(\text{C}_{30}\text{H}_{34}\text{N}_4\text{O}_2)(\text{I})_2$

C, 42.20 ; H, 4.01 ; N, 6.56

Found(%) C, 43.10 ; H, 4.18 ; N, 6.88

Solubility : MeOH, DMSO, DMF, Acetonitrile

λ_M (DMSO) : $68.1 \text{ ohm}^{-1}\text{cm}^2\text{mol}^{-1}$

3) Preparation of mononuclear Ni(II) complexes

(1) $[\text{Ni}(\text{H}_2[\text{20}]\text{-DCHDC})](\text{ClO}_4)_2 \cdot 2\text{H}_2\text{O}$

Nickel perchloride hexahydrate (21.94 g), 2,6-diformyl-*p*-cresol (4.92 g), and *trans*-1,2-diaminocyclohexane (3.42 g) in methanol (200 mL) were refluxed

for 1 day. The solution was concentrated under rota evaporation to approximate 50 mL and then it was on standing overnight at room temperature. The resulting red-brown precipitate was filtered, thoroughly washed twice with methanol, dried under vacuum over anhydrous calcium chloride (Scheme 2).

Yield : 6.7499 g (57.8%)

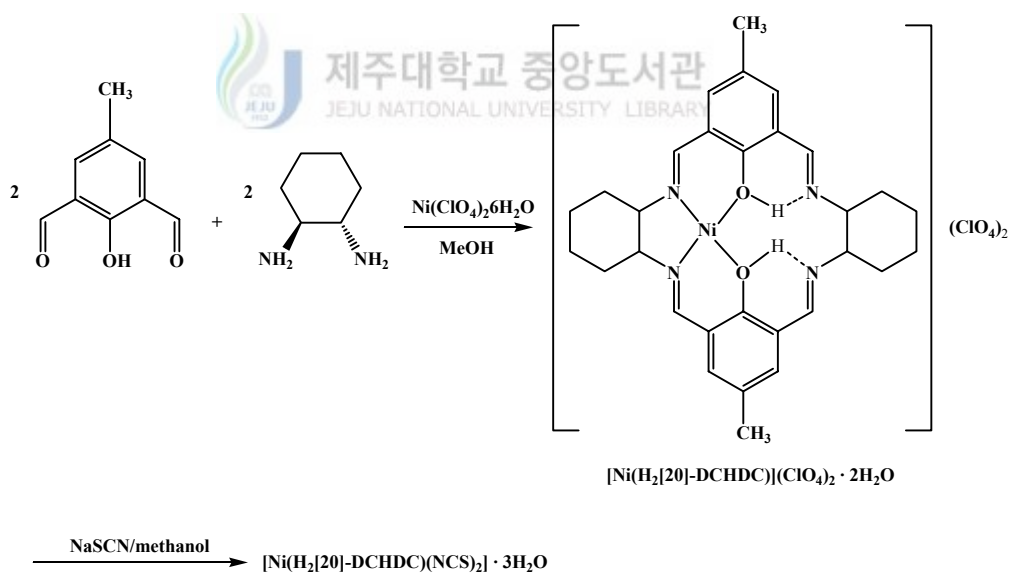
Anal. Calc.(%) for $\text{Ni}(\text{C}_{30}\text{H}_{36}\text{N}_4\text{O}_2)(\text{ClO}_4)_2(\text{H}_2\text{O})_2$

C, 46.30 ; H, 5.18 ; N, 7.20

Found(%) C, 46.28 ; H, 4.85 ; N, 7.12

Solubility : MeOH, DMSO, DMF, Acetonitrile

λ_M (Acetonitrile) : $322 \text{ ohm}^{-1}\text{cm}^2\text{mol}^{-1}$



Scheme 2. Synthesis of the mononuclear Ni(II) complexes of phenol-based macrocyclic ligand.

(2) [Ni(H₂[20]-DCHDC)(NCS)₂] · 3H₂O

A solution of [Ni(H₂[20]-DCHDC)](ClO₄)₂(H₂O)₂ (0.778 g) in methanol (150 mL) was added dropwise of sodium thiocyanide (0.8107 g) with stirring and the mixture was refluxed whereupon the initial red-brown precipitate first turned dark orange. The resulting red-brown precipitate were filtered, thoroughly washed twice with water, and dried under vacuum.

Yield : 0.5554 g (77.5%)

Anal. Calc.(%) for Ni(C₃₀H₃₆N₄O₂)(NCS)₂(H₂O)₃

C, 53.87 ; H, 5.93 ; N, 11.78

Found(%) C, 53.99 ; H, 5.29 ; N, 11.11

Solubility : MeOH, DMSO, DMF, Acetonitrile

λ_M (DMSO) : 76.2 ohm⁻¹cm²mol⁻¹



3. X-ray Diffraction Measurements

1) $[\text{Ni}_2([\text{20}]\text{-DCHDC})](\text{ClO}_4)_2 \cdot 2\text{CH}_3\text{CN}$

Suitable crystals of $[\text{Ni}_2([\text{20}]\text{-DCHDC})](\text{ClO}_4)_2 \cdot 2\text{CH}_3\text{CN}$ were obtained by slow evaporation of acetonitrile solutions of $[\text{Ni}_2([\text{20}]\text{-DCHDC})](\text{ClO}_4)_2$ complex at atmospheric pressure. The dark brown crystal of $[\text{Ni}_2([\text{20}]\text{-DCHDC})](\text{ClO}_4)_2 \cdot 2\text{CH}_3\text{CN}$ was attached to glass fibers and mounted on a Bruker SMART diffractometer equipped with a graphite monochromated Mo $K\alpha$ ($= 0.71073 \text{ \AA}$) radiation, operating at 50 kV and 30 mA and a CCD detector, 45 frames of two-dimensional diffraction images were collected and processed to obtain the cell parameters and orientation matrix. The crystallographic data, conditions for the collection of intensity data, and some features of the structure refinements are listed in Table 1, and atomic coordinates were given in Table 2. The intensity data were corrected for Lorentz and polarization effects. Absorption correction was not made during processing. Of the 10649 unique reflections measured, 3834 reflections in the range $2.15^\circ \leq \theta \leq 26.37^\circ$ were considered to be observed ($I > 2\sigma(I)$) and were used in subsequent structure analysis. The program SAINTPLUS²³ was used for integration of the diffraction profiles. The structures were solved by direct methods using the SHELXS program of the SHELXTL package and refined by full matrix least squares against F^2 for all data using SHELXL. All non-H atoms were refined with anisotropic displacement parameters (Table 3). Hydrogen atoms were placed in idealized positions [$U_{\text{iso}} = 1.2U_{\text{eq}}$ (parent atom)]. Hydrogen coordinates and isotropic displacement parameters were given in Table 4.

Table 1. Crystal data and structure refinement for $[\text{Ni}_2([\text{20}]\text{-DCHDC})](\text{ClO}_4)_2 \cdot 2\text{CH}_3\text{CN}$ complex.

Empirical formula	$\text{C}_{34}\text{H}_{40}\text{Cl}_2\text{N}_6\text{Ni}_2\text{O}_{10}$ $[\text{Ni}_2(\text{C}_{30}\text{H}_{34}\text{N}_4\text{O}_2)](\text{ClO}_4)_2(\text{CH}_3\text{CN})_2$	
Formula weight	881.04	
Temperature	173(2) K	
Wavelength	0.71073 Å	
Crystal system	Monoclinic	
Space group	$P_2(1)/c$	
Unit cell dimensions	$a = 9.2745(5)$ Å	$a = 90^\circ$.
	$b = 18.9687(10)$ Å	$\beta = 104.1230(10)^\circ$.
	$c = 11.0198(6)$ Å	$\gamma = 90^\circ$.
Volume	$1880.06(17)$ Å ³	
Z	2	
Density (calculated)	1.556 g/cm ³	
Absorption coefficient	1.208 mm ⁻¹	
$F(000)$	912	
Crystal size	0.40 x 0.30 x 0.30 mm ³	
Theta range for data collection	2.15 to 26.37°	
Index ranges	$-11 \leq h \leq 9$, $-23 \leq k \leq 21$, $-13 \leq l \leq 13$	
Reflections collected	10649	
Independent reflections	3834 [$R(\text{int}) = 0.0392$]	
Completeness to theta = 26.37°	99.7 %	
Absorption correction	None	
Refinement method	Full-matrix least-squares on F^2	
Data / restraints / parameters	3834 / 0 / 245	
Goodness-of-fit on F^2	1.071	
Final R indices [$I > 2\sigma(I)$]	$R_1 = 0.0580$, $wR_2 = 0.1507$	
R indices (all data)	$R_1 = 0.0743$, $wR_2 = 0.1622$	

$$R = \frac{\sum \|F_o\| - |F_c|}{\sum \|F_o\|}, \quad R_w = \left[\frac{\sum w(F_o^2 - F_c^2)^2}{\sum w(F_o^2)^2} \right]^{1/2}$$

$$w = 1 / [\sigma^2(F_o^2) + (0.0382P)^2 + 7.0524P] \quad \text{where } P = (F_o^2 + 2F_c^2) / 3.$$

Table 2. Atomic coordinates ($\times 10^4$) and equivalent isotropic displacement parameters ($\text{\AA}^2 \times 10^3$) for $[\text{Ni}_2([\text{20}]\text{-DCHDC})](\text{ClO}_4)_2 \cdot 2\text{CH}_3\text{CN}$ complex

	<i>x</i>	<i>y</i>	<i>z</i>	$U_{(\text{eq})}$
Ni(1)	-83(1)	4294(1)	5361(1)	28(1)
O(1)	1192(3)	4891(2)	4812(3)	35(1)
N(1)	1079(4)	3512(2)	5409(3)	30(1)
N(2)	-1420(4)	3760(2)	5931(4)	32(1)
C(1)	2332(4)	4735(2)	4335(4)	27(1)
C(2)	3017(4)	5268(2)	3772(4)	29(1)
C(3)	4214(5)	5083(2)	3273(4)	30(1)
C(4)	4746(5)	4395(2)	3312(4)	32(1)
C(5)	4089(4)	3888(2)	3892(4)	31(1)
C(6)	2885(4)	4040(2)	4411(4)	28(1)
C(7)	2257(5)	3472(2)	5005(4)	30(1)
C(8)	566(6)	2939(3)	6119(6)	50(1)
C(9)	1093(5)	2199(2)	5932(5)	39(1)
C(10)	425(7)	1686(3)	6696(8)	75(2)
C(11)	-1154(7)	1759(3)	6586(8)	67(2)
C(12)	-1717(5)	2501(2)	6700(5)	40(1)
C(13)	-1049(6)	2995(2)	5890(6)	51(1)
C(14)	-2555(5)	3999(2)	6283(4)	33(1)
C(15)	6030(5)	4211(3)	2742(5)	42(1)
Cl(1)	4819(1)	3189(1)	8617(1)	45(1)
O(2)	4575(7)	3249(3)	7294(5)	100(2)
O(3)	5404(7)	3824(3)	9190(5)	92(2)
O(4)	3506(6)	2970(3)	8926(6)	98(2)
O(5)	5919(6)	2636(3)	8949(6)	100(2)
N(3)	497(9)	4744(4)	8071(8)	113(3)
C(16)	1423(7)	4722(3)	8967(7)	64(2)
C(17)	2595(7)	4724(4)	10076(6)	65(2)

$U_{(\text{eq})}$ is defined as one third of the trace of the orthogonalized U^{ij} tensor.

Table 3. Anisotropic displacement parameters ($\text{\AA}^2 \times 10^3$) for $[\text{Ni}_2([\text{20}]\text{-DCHDC})](\text{ClO}_4)_2 \cdot 2\text{CH}_3\text{CN}$ complex

	U^{11}	U^{22}	U^{33}	U^{23}	U^{13}	U^{12}
Ni(1)	27(1)	23(1)	37(1)	1(1)	16(1)	-1(1)
O(1)	36(2)	24(1)	56(2)	7(1)	29(2)	2(1)
N(1)	31(2)	24(2)	37(2)	3(2)	14(2)	1(1)
N(2)	32(2)	23(2)	45(2)	2(2)	19(2)	-2(1)
C(1)	22(2)	27(2)	34(2)	1(2)	12(2)	0(2)
C(2)	26(2)	27(2)	36(2)	1(2)	13(2)	-1(2)
C(3)	28(2)	32(2)	34(2)	1(2)	13(2)	-3(2)
C(4)	28(2)	37(2)	36(2)	1(2)	14(2)	3(2)
C(5)	26(2)	29(2)	41(2)	-3(2)	13(2)	2(2)
C(6)	25(2)	27(2)	33(2)	0(2)	11(2)	-2(2)
C(7)	29(2)	25(2)	38(2)	3(2)	12(2)	4(2)
C(8)	52(3)	33(2)	73(4)	16(3)	35(3)	6(2)
C(9)	36(2)	28(2)	56(3)	9(2)	21(2)	4(2)
C(10)	73(4)	44(3)	126(6)	38(4)	61(4)	18(3)
C(11)	57(3)	32(3)	129(6)	27(3)	52(4)	4(2)
C(12)	38(2)	34(2)	56(3)	11(2)	25(2)	1(2)
C(13)	48(3)	27(2)	89(4)	10(3)	39(3)	3(2)
C(14)	31(2)	29(2)	42(2)	7(2)	18(2)	-2(2)
C(15)	37(2)	43(3)	54(3)	2(2)	27(2)	2(2)
Cl(1)	47(1)	38(1)	50(1)	6(1)	12(1)	-14(1)
O(2)	99(4)	117(5)	78(4)	10(3)	10(3)	-41(4)
O(3)	126(4)	58(3)	90(4)	-15(3)	24(3)	-38(3)
O(4)	100(4)	64(3)	159(6)	5(3)	86(4)	-14(3)
O(5)	64(3)	72(3)	152(6)	9(4)	2(3)	1(3)
N(3)	91(5)	98(5)	121(6)	-34(5)	-28(5)	-2(4)
C(16)	56(4)	51(3)	79(4)	-16(3)	6(3)	-7(3)
C(17)	54(4)	68(4)	65(4)	-5(3)	3(3)	-15(3)

The anisotropic displacement factor exponent takes the form: $-2\pi^2[h^2 a^{*2}U^{11} + \dots + 2 hka^* b^* U^{12}]$.

Table 4. Hydrogen coordinates ($\times 10^4$) and isotropic displacement parameters ($\text{\AA}^2 \times 10^3$) for $[\text{Ni}_2([\text{20}]\text{-DCHDC})](\text{ClO}_4)_2 \cdot 2\text{CH}_3\text{CN}$ complex

	<i>x</i>	<i>y</i>	<i>z</i>	<i>U</i> _(eq)
H(3)	4679	5439	2895	36
H(5)	4463	3420	3943	38
H(7)	2767	3034	5102	36
H(8)	973	3052	7024	60
H(9A)	785	2070	5035	46
H(9B)	2191	2177	6200	46
H(10A)	619	1201	6445	90
H(10B)	948	1743	7588	90
H(11A)	-1421	1463	7239	81
H(11B)	-1689	1566	5764	81
H(12A)	-1425	2657	7584	48
H(12B)	-2816	2511	6421	48
H(13)	-1460	2841	5006	61
H(14)	-3136	3668	6605	39
H(15A)	6256	3707	2859	50
H(15B)	6907	4487	3153	50
H(15C)	5757	4321	1846	50
H(17A)	3163	5162	10121	78
H(17B)	3254	4321	10063	78
H(17C)	2175	4688	10808	78

2) [Ni(H₂[20]-DCHDC)](ClO₄)₂

Suitable crystals of [Ni(H₂[20]-DCHDC)](ClO₄)₂ were obtained by slow evaporation of methanol solutions of [Ni(H₂[20]-DCHDC)](ClO₄)₂·2H₂O complex at atmospheric pressure. The dark green crystal of [Ni(H₂[20]-DCHDC)](ClO₄)₂ was attached to glass fibers and mounted on a Bruker SMART diffractometer equipped with a graphite monochromated Mo K α ($= 0.71073 \text{ \AA}$) radiation, operating at 50 kV and 30 mA and a CCD detector ; 45 frames of two-dimensional diffraction images were collected and processed to obtain the cell parameters and orientation matrix. The crystallographic data, conditions for the collection of intensity data, and some features of the structure refinements are listed in Table 5, and atomic coordinates were given in Table 6. The intensity data were corrected for Lorentz and polarization effects. Absorption correction was not made during processing. Of the 9011 unique reflections measured, 3205 reflections in the range $2.23^\circ \leq \theta \leq 26.37^\circ$ were considered to be observed ($I > 2\sigma(I)$) and were used in subsequent structure analysis. The program SAINTPLUS was used for integration of the diffraction profiles. The structures were solved by direct methods using the SHELXS program²³ of the SHELXTL package and refined by full matrix least squares against F^2 for all data using SHELXL. All non-H atoms were refined with anisotropic displacement parameters (Table 7). Hydrogen atoms were placed in idealized positions [$U_{\text{iso}} = 1.2U_{\text{eq}}$ (parent atom)]. Hydrogen coordinates and isotropic displacement parameters were given in Table 8.

Table 5. Crystal data and structure refinement for [Ni(H₂[20]-DCHDC)](ClO₄)₂ complex

Empirical formula	C ₃₀ H ₃₆ Cl ₂ N ₄ NiO ₁₀ [Ni(C ₃₀ H ₃₆ N ₄ O ₂)](ClO ₄) ₂	
Formula weight	742.24	
Temperature	173(2) K	
Wavelength	0.71073 Å	
Crystal system	Monoclinic	
Space group	P2(1)/n	
Unit cell dimensions	$a = 9.2033(5)$ Å	$a = 90^\circ$.
	$b = 14.6208(8)$ Å	$\beta = 99.8950(10)^\circ$
	$c = 11.8316(7)$ Å	$\gamma = 90^\circ$.
Volume	1568.37(15) Å ³	
Z	2	
Density (calculated)	1.572 g/cm ³	
Absorption coefficient	0.854 mm ⁻¹	
F(000)	772	
Crystal size	0.15 x 0.15 x 0.10 mm ³	
Theta range for data collection	2.23 to 26.37° .	
Index ranges	-11<=h<=11, -18<=k<=17, -14<=l<=8	
Reflections collected	9011	
Independent reflections	3205 [R(int) = 0.0666]	
Completeness to theta = 28.29°	99.8 %	
Absorption correction	None	
Refinement method	Full-matrix least-squares on F ²	
Data / restraints / parameters	3205 / 0 / 217	
Goodness-of-fit on F ²	1.176	
Final R indices [I>2σ(I)]	R ₁ = 0.0811, wR ₂ = 0.1984	
R indices (all data)	R ₁ = 0.1149, wR ₂ = 0.2142	

$$R = \frac{\sum \|F_o\| - |F_c|}{\sum |F_o|}, \quad R_w = \left[\frac{\sum w(F_o^2 - F_c^2)^2}{\sum w(F_o^2)^2} \right]^{1/2}$$

$$w = 1/[\sigma^2(F_o^2) + (0.0404P)^2 + 7.2146P] \quad \text{where } P = (F_o^2 + 2F_c^2)/3.$$

Table 6. Atomic coordinates ($\times 10^4$) and equivalent isotropic displacement parameters ($\text{\AA}^2 \times 10^3$) for $[\text{Ni}(\text{H}_2[20]\text{-DCHDC})](\text{ClO}_4)_2$ complex

	<i>x</i>	<i>y</i>	<i>z</i>	$U_{\text{(eq)}}$
Ni(1)	936(1)	84(1)	4290(1)	18(1)
Cl(1)	2574(2)	2831(1)	4503(2)	50(1)
O(1)	-873(4)	511(3)	4443(4)	40(1)
O(2)	3191(6)	1965(4)	4949(5)	67(2)
O(3)	1178(6)	2965(5)	4815(6)	80(2)
O(4)	3554(6)	3560(4)	4966(5)	70(2)
O(5)	2472(7)	2829(4)	3271(5)	67(2)
N(1)	877(6)	726(4)	2880(5)	43(1)
N(2)	2774(6)	-371(4)	4107(4)	41(1)
C(1)	-1582(6)	1256(4)	4019(5)	31(1)
C(2)	-2793(6)	1586(4)	4493(5)	34(1)
C(3)	-3516(6)	2381(4)	4034(6)	38(1)
C(4)	-3102(7)	2845(4)	3140(6)	45(2)
C(5)	-1943(7)	2511(4)	2658(6)	43(2)
C(6)	-1172(6)	1715(4)	3090(5)	35(1)
C(7)	42(6)	1423(4)	2552(6)	39(1)
C(8)	2086(7)	376(5)	2292(6)	44(2)
C(9)	2515(7)	1011(5)	1392(6)	44(2)
C(10)	3815(8)	601(6)	909(7)	58(2)
C(11)	5051(8)	376(6)	1819(6)	59(2)
C(12)	4649(7)	-246(5)	2752(6)	42(2)
C(13)	3388(7)	184(5)	3246(6)	48(2)
C(14)	3348(7)	-1110(4)	4595(5)	36(1)
C(15)	-3910(9)	3693(6)	2649(9)	75(3)

$U_{\text{(eq)}}$ is defined as one third of the trace of the orthogonalized U^{ij} tensor.

Table 7. Anisotropic displacement parameters ($\text{\AA}^2 \times 10^3$) for $[\text{Ni}(\text{H}_2[20]-\text{DCHDC})](\text{ClO}_4)_2$ complex

	U^{11}	U^{22}	U^{33}	U^{23}	U^{13}	U^{12}
Ni(1)	15(1)	19(1)	19(1)	2(1)	6(1)	5(1)
Cl(1)	37(1)	58(1)	55(1)	-14(1)	6(1)	13(1)
O(1)	35(2)	39(2)	49(3)	9(2)	13(2)	14(2)
O(2)	79(4)	57(3)	69(4)	-4(3)	24(3)	22(3)
O(3)	38(3)	108(5)	95(5)	-24(4)	18(3)	14(3)
O(4)	55(3)	75(4)	73(4)	-21(3)	-10(3)	6(3)
O(5)	81(4)	70(4)	48(3)	-14(3)	3(3)	4(3)
N(1)	41(3)	40(3)	55(4)	10(3)	25(3)	6(2)
N(2)	40(3)	50(3)	37(3)	5(2)	17(2)	11(2)
C(1)	27(3)	29(3)	38(3)	-1(2)	4(2)	2(2)
C(2)	27(3)	34(3)	42(4)	-4(3)	7(3)	6(2)
C(3)	30(3)	38(3)	47(4)	2(3)	8(3)	7(3)
C(4)	36(3)	39(3)	61(5)	11(3)	11(3)	6(3)
C(5)	33(3)	45(4)	51(4)	10(3)	9(3)	0(3)
C(6)	27(3)	36(3)	42(4)	0(3)	8(2)	0(2)
C(7)	28(3)	47(4)	43(4)	8(3)	11(3)	1(3)
C(8)	39(3)	55(4)	41(4)	6(3)	16(3)	11(3)
C(9)	47(4)	45(4)	43(4)	8(3)	18(3)	4(3)
C(10)	53(4)	68(5)	59(5)	8(4)	28(4)	-1(4)
C(11)	50(4)	81(6)	54(5)	5(4)	34(4)	4(4)
C(12)	35(3)	51(4)	42(4)	-2(3)	16(3)	5(3)
C(13)	40(4)	55(4)	50(4)	2(3)	14(3)	-1(3)
C(14)	34(3)	37(3)	39(4)	0(3)	10(3)	10(3)
C(15)	62(5)	63(5)	107(7)	38(5)	33(5)	33(4)

The anisotropic displacement factor exponent takes the form: $-2\pi^2[h^2 a^{*2}U^{11} + \dots + 2 hka^* b^* U^{12}]$.

Table 8. Hydrogen coordinates ($\times 10^4$) and isotropic displacement parameters ($\text{\AA}^2 \times 10^3$) for $[\text{Ni}(\text{H}_2[20]\text{-DCHDC})](\text{ClO}_4)_2$ complex

	x	y	z	$U_{(\text{eq})}$
H(3)	-4324	2605	4357	46
H(5)	-1661	2823	2025	51
H(7)	242	1765	1914	46
H(8)	1756	-218	1913	53
H(9A)	2796	1616	1738	52
H(9B)	1664	1098	765	52
H(10A)	3484	40	471	69
H(10B)	4149	1043	374	69
H(11A)	5467	952	2178	71
H(11B)	5830	75	1469	71
H(12A)	4348	-854	2426	50
H(12B)	5516	-328	3367	50
H(13)	3740	780	3609	57
H(14)	4189	-1357	4338	44
H(15A)	-4699	3836	3082	90
H(15B)	-4338	3587	1842	90
H(15C)	-3219	4207	2703	90

III. Results and Discussion

1. IR spectra of the complexes

IR spectra of the nickel complexes were presented in Figure 1 ~ 8. The characteristics of the complexes were listed in Table 1 and 2. The strong and sharp absorption bands occurring at $1620 \sim 1652 \text{ cm}^{-1}$ are attributed to $\nu(\text{C}=\text{N})$ of the coordinated [20]-DCHDC ligand,^{24,25} and the absence of any carbonyl bands associated with the diformylphenol starting materials or nonmacrocyclic intermediates. The IR spectra displayed three C-H stretching vibrations from 3000 to 2800 cm^{-1} . A strong bands at near $\sim 1550 \text{ cm}^{-1}$ region associated with the aromatic ring C=C vibrations. The sharp absorption bands occurring at $\sim 1230 \text{ cm}^{-1}$ regions are attributed to phenolic C-O stretching vibration. The present complexes exhibited four C-H deformation bands at 1450 , 1380 , 1350 and 1320 cm^{-1} regions and three out-of-plan vibration bands at 860 , 820 and 770 cm^{-1} regions. The bands occurring in the IR spectra of the complexes in the $3500 \sim 3300 \text{ cm}^{-1}$ regions may probably be due to the $\nu(\text{OH})$ vibration of the lattice water. A strong ionic ClO_4^- band at near 1107 cm^{-1} and 622 cm^{-1} in $[\text{Ni}_2([\text{20}]\text{-DCHDC})](\text{ClO}_4)_2$ complex.

The thiocyanate ion may act as an ambidentate ligand, bonding may occur either through the nitrogen or the sulphur atom. The bonding mode may easily be distinguished by examining the band due to the C-S stretching vibration which occurs at $730\text{-}690 \text{ cm}^{-1}$ when the bonding occurs through the sulphur atom and at $860\text{-}780 \text{ cm}^{-1}$ when it is through the nitrogen atom.²⁶ The $\text{C}\equiv\text{N}$ stretching vibration of thiocyanato-complexes Ga-NCS (i.e. nitrogen bound), the resulting band is strong and occurs in the region 2044 cm^{-1} . The

absorption vibrations due to the N-coordinated bonded NCS^- in $[\text{Ni}_2([\text{20}]\text{-DCHDC})(\text{NCS})_2]$ appear 2044 and 871 cm^{-1} .

In general, for azides the band due to the asymmetric N_3 stretching vibration is strong and occurs in the region 2015 cm^{-1} , while that due to the symmetric vibration is much weaker and occurs in the region $1379\text{-}1238\text{ cm}^{-1}$ and the band due to the deformation vibration is also weak and occurs at $680\text{-}410\text{ cm}^{-1}$.²⁷ The absorption peak at 2015 cm^{-1} in the $[\text{Ni}_2([\text{20}]\text{-DCHDC})(\text{N}_3)_2]$ is assigned to the asymmetric stretching mode of coordinated azide. The symmetric stretching frequency of coordinated azide is observed at 1346 cm^{-1} .

Linkage isomerism is possible in the case of metal complexes containing the unit NO_2 . Coordination to the metal atom may occur through the nitrogen atom, resulting in a nitro-complex, or through an oxygen atom, resulting in a nitrito-complex. Nitro-complexes exhibit bands due to asymmetric and symmetric $-\text{NO}_2$ stretching vibration and, in addition, one due to a NO_2 deformation vibration.²⁷ The nitrito-complexes exhibit bands due to asymmetric and symmetric $-\text{ONO}$ stretching vibrations which are well separated and occur at $1485\text{-}1400\text{ cm}^{-1}$ and $1110\text{-}1050\text{ cm}^{-1}$, respectively. Nitro-groups in metal coordination complexes may exist as bridging or as end groups. Terminal nitro-groups absorb at $1485\text{-}1370\text{ cm}^{-1}$ and $1340\text{-}1315\text{ cm}^{-1}$ due to the asymmetric and symmetric stretching vibrations of the NO_2 group, respectively.^{28,29} Nitrito-complexes do not have a band near 620 cm^{-1} which is present for all nitro-complexes. Nitro-groups acting as bridging units (M-ONO-M) between two metal atoms absorb at $1485\text{-}1470\text{ cm}^{-1}$ and at about 1200 cm^{-1} , these bands being broader than those for terminal nitro-groups.²⁶ The strong absorption peaks at 1450 and 1238 cm^{-1} in the $[\text{Ni}_2([\text{20}]\text{-DCHDC})(\mu\text{-ONO})]\text{NO}_2 \cdot 1.5\text{H}_2\text{O}$ are assigned to a bridging bidentate ligand Ni-ONO-Ni. And stretching bands of NO_2 counter ion are observed at

1327 and 1272 cm^{-1} . A strong ionic ClO_4^- band at near 1089 cm^{-1} and 622 cm^{-1} in $[\text{Ni}(\text{H}_2[20]\text{-DCHDC})](\text{ClO}_4)_2 \cdot 2\text{H}_2\text{O}$ complex. The absorption vibrations due to the N-coordinated bonded NCS^- in $[\text{Ni}(\text{H}_2[20]\text{-DCHDC})(\text{NCS})_2] \cdot 3\text{H}_2\text{O}$ appear 2044 and 869 cm^{-1} .



Table 9. Characteristic IR absorptions (cm^{-1}) of macrocyclic ligand ($\text{H}_2[20]\text{-DCHDC}$) for the Ni(II) complexes

Compounds	Assignments					
	Macrocycle					
	$\nu(\text{CH})$	$\nu(\text{C=N})$	$\nu(\text{C=C})$	$\nu(\text{C-O})$		
$[\text{Ni}_2([20]\text{-DCHDC})\text{Cl}_2]$	3003	2939	2864	1625	1560	1242
$[\text{Ni}_2([20]\text{-DCHDC})](\text{ClO}_4)_2$	3045	2945	2862	1624	1562	1242
$[\text{Ni}_2([20]\text{-DCHDC})(\text{NCS})_2]$	3028	2941	2862	1624	1556	1234
$[\text{Ni}_2([20]\text{-DCHDC})(\text{N}_3)_2]$	3016	2931	2860	1625	1541	1240
$[\text{Ni}_2([20]\text{-DCHDC})(\mu\text{-ONO})]\text{NO}_2 \cdot 1.5\text{H}_2\text{O}$	3016	2933	2860	1627	1542	1240
$[\text{Ni}_2([20]\text{-DCHDC})\text{I}_2]$	2999	2939	2856	1620	1558	1240
$[\text{Ni}(\text{H}_2[20]\text{-DCHDC})](\text{ClO}_4)_2 \cdot 2\text{H}_2\text{O}$	3041	2939	2864	1635	1558	1240
$[\text{Ni}(\text{H}_2[20]\text{-DCHDC})(\text{NCS})_2] \cdot 3\text{H}_2\text{O}$	3030	2939	2860	1635	1556	1234

Table 1. *continued*

Compounds	Assignments							
	Macrocycle							
	$\bar{\nu}(\text{CH})$				$\bar{\nu}_{\text{oop}}(\text{CH})$			
$[\text{Ni}_2([\text{20}]\text{-DCHDC})\text{Cl}_2$	1452	1386	1344	1326	871	823	767	
$[\text{Ni}_2([\text{20}]\text{-DCHDC})](\text{ClO}_4)_2$	1460	1388	1348	1328	873	842	757	
$[\text{Ni}_2([\text{20}]\text{-DCHDC})(\text{NCS})_2]$	1454	1388	1344	1307	867	821	757	
$[\text{Ni}_2([\text{20}]\text{-DCHDC})(\text{N}_3)_2]$	1450	1388	1346	1301	869	829	767	
$[\text{Ni}_2([\text{20}]\text{-DCHDC})(\mu\text{-ONO})]\text{NO}_2 \cdot 1.5\text{H}_2\text{O}$	1452	1388	1348	1301	869	829	765	
$[\text{Ni}_2([\text{20}]\text{-DCHDC})\text{I}_2]$	1454	1382	1346	1309	871	823	757	
$[\text{Ni}(\text{H}_2[\text{20}]\text{-DCHDC})](\text{ClO}_4)_2 \cdot 2\text{H}_2\text{O}$	1450	1384	1353	1311	866	821	771	
$[\text{Ni}(\text{H}_2[\text{20}]\text{-DCHDC})(\text{NCS})_2] \cdot 3\text{H}_2\text{O}$	1444	1386	1355	1309	869	823	771	

Table 10. Characteristic IR absorptions (cm^{-1}) of exocyclic molecules for the Ni(II) complexes

Compounds	Assignments
$[\text{Ni}_2([20]\text{-DCHDC})\text{Cl}_2]$	
$[\text{Ni}_2([20]\text{-DCHDC})](\text{ClO}_4)_2$	1107(br), 622 $\nu(\text{ClO}_4^-)$ ionic
$[\text{Ni}_2([20]\text{-DCHDC})(\text{NCS})_2]$	2044 (vs) ; $\nu(\text{C}=\text{N})$ N-bonded NCS^- ; 874(w) ; $\nu(\text{C}-\text{S})$ N-bonded NCS^-
$[\text{Ni}_2([20]\text{-DCHDC})(\text{N}_3)_2]$	3440 (br) ; $\nu(\text{OH})$ lattice H_2O 2015 (vs) ; $\nu_{\text{as}}(\text{NNN})$ coord. N_3^- ; 1238 (m) ; $\nu_{\text{s}}(\text{NNN})$ coord. N_3^- ;
$[\text{Ni}_2([20]\text{-DCHDC})\text{I}_2]$	
$[\text{Ni}_2([20]\text{-DCHDC})(\mu\text{-ONO})]\text{NO}_2 \cdot 1.5\text{H}_2\text{O}$	3438 $\nu(\text{OH})$ lattice H_2O 1450(s), 1238(m); bridging NO_2 , Ni-ONO-Ni 1348 (s), 1272(m) ; ionic NO_2^-
$[\text{Ni}(\text{H}_2[20]\text{-DCHDC})](\text{ClO}_4)_2 \cdot 2\text{H}_2\text{O}$	3336 (br) ; $\nu(\text{OH})$ lattice H_2O 1089(br), 622 $\nu(\text{ClO}_4^-)$ ionic
$[\text{Ni}(\text{H}_2[20]\text{-DCHDC})(\text{NCS})_2] \cdot 3\text{H}_2\text{O}$	3425 (br) ; $\nu(\text{OH})$ lattice H_2O 2044 (br, vs) ; $\nu(\text{C}=\text{N})$ N-bonded NCS^- ; 869(w) ; $\nu(\text{C}-\text{S})$ N-bonded NCS^-

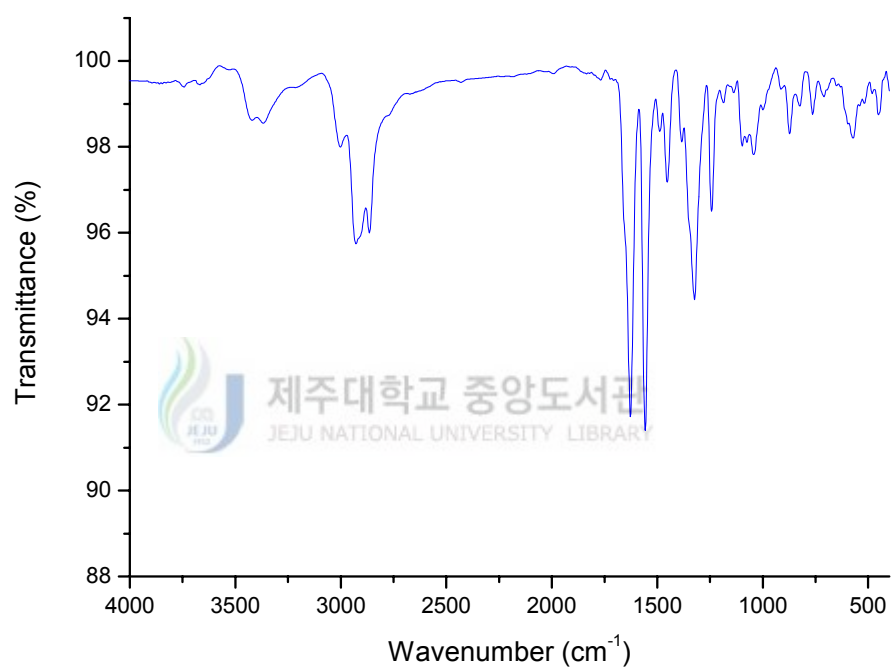


Figure 1. FT-IR spectrum of [Ni₂([20]-DCHDC)]Cl₂ complex.

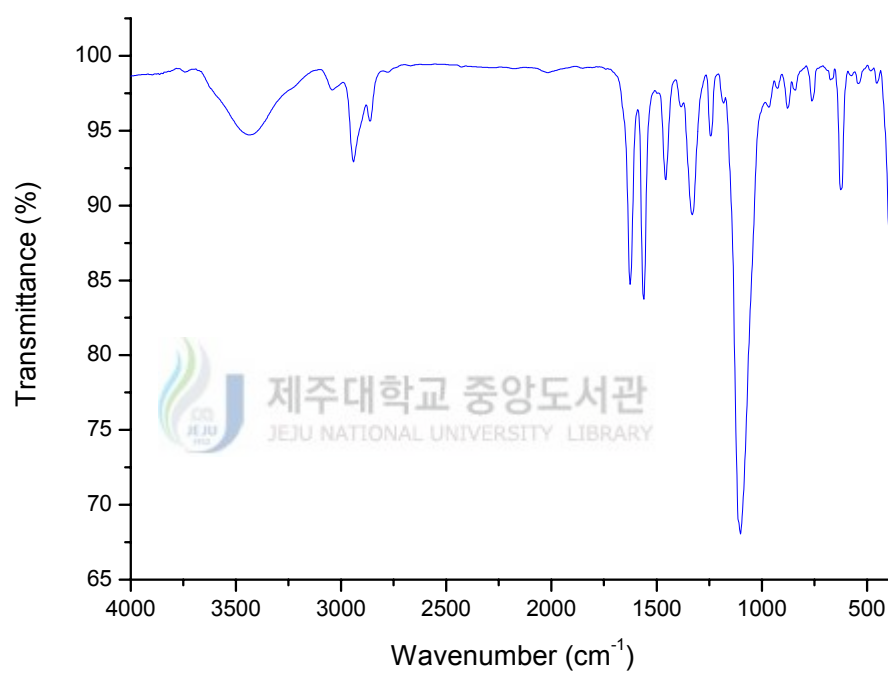


Figure 2. FT-IR spectrum of [Ni₂([20]-DCHDC)](ClO₄)₂ complex.

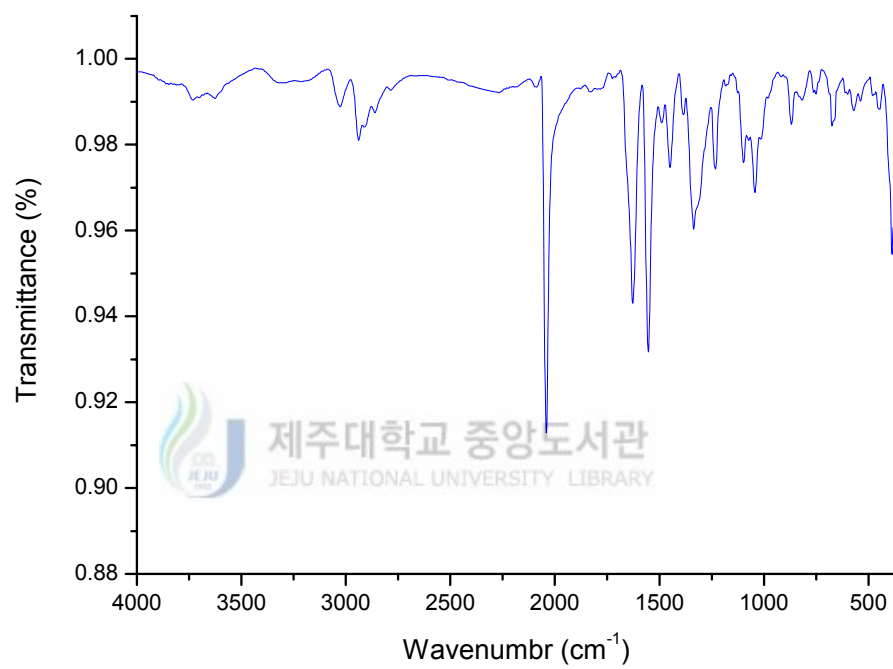


Figure 3. FT-IR spectrum of $[\text{Ni}_2([\text{20}]\text{-DCHDC})(\text{NCS})_2]$ complex.

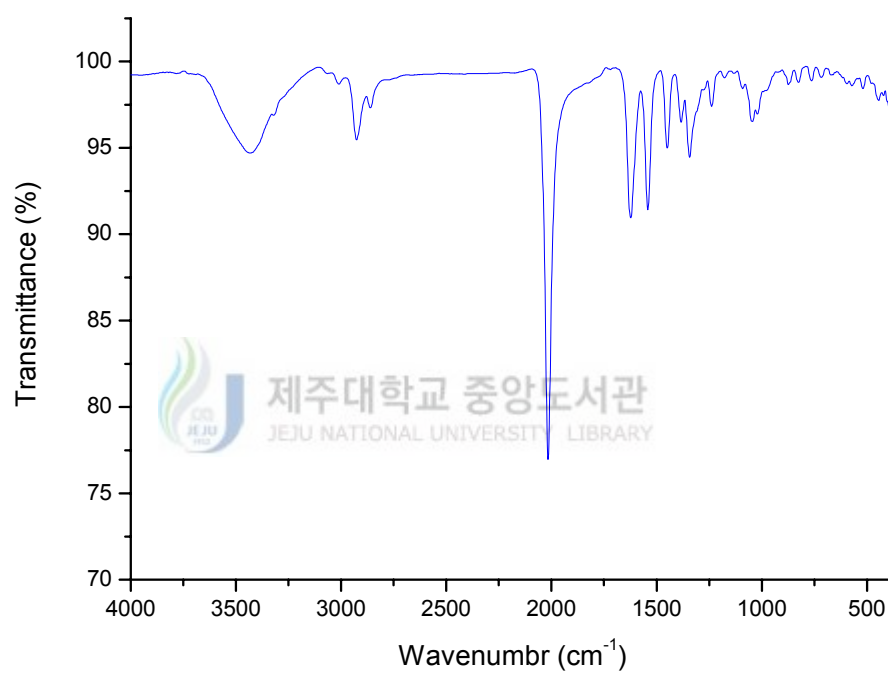


Figure 4. FT-IR spectrum of [Ni₂([20]-DCHDC)(N₃)₂] complex.

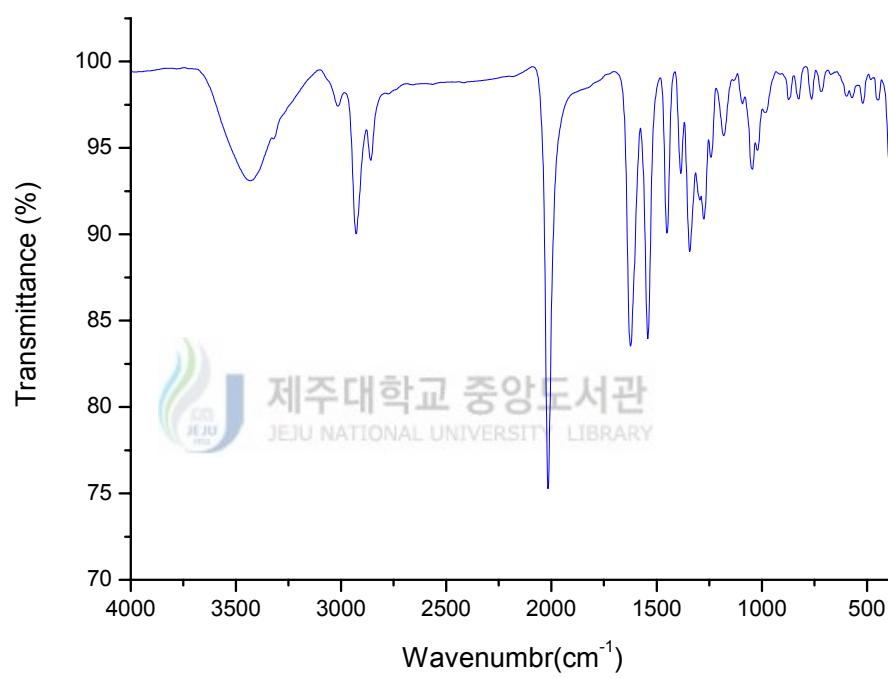


Figure 5. FT-IR spectrum of $[\text{Ni}_2([\text{20}]\text{-DCHDC})(\mu\text{-ONO})]\text{NO}_2 \cdot 1.5\text{H}_2\text{O}$ complex.

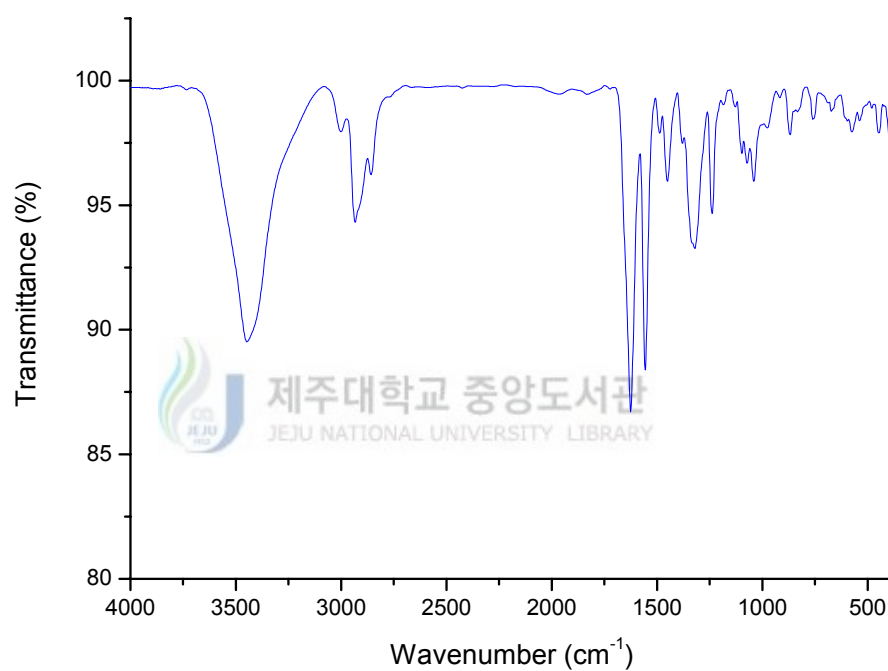


Figure 6. FT-IR spectrum of [Ni₂([20]-DCHDC)I₂] complex.

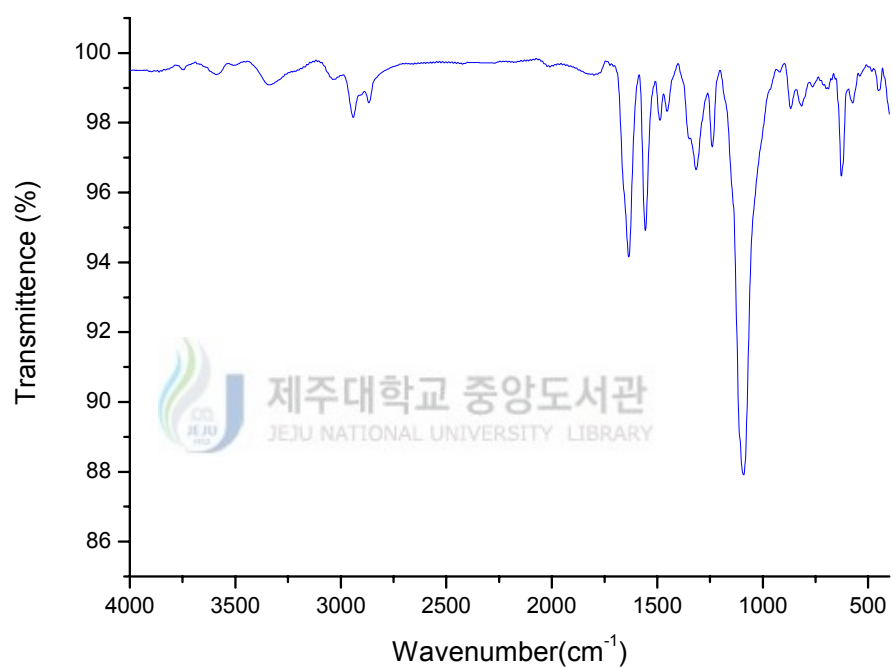


Figure 7. FT-IR spectrum of [Ni(H₂[20]-DCHDC)](ClO₄)₂ · 2H₂O complex.

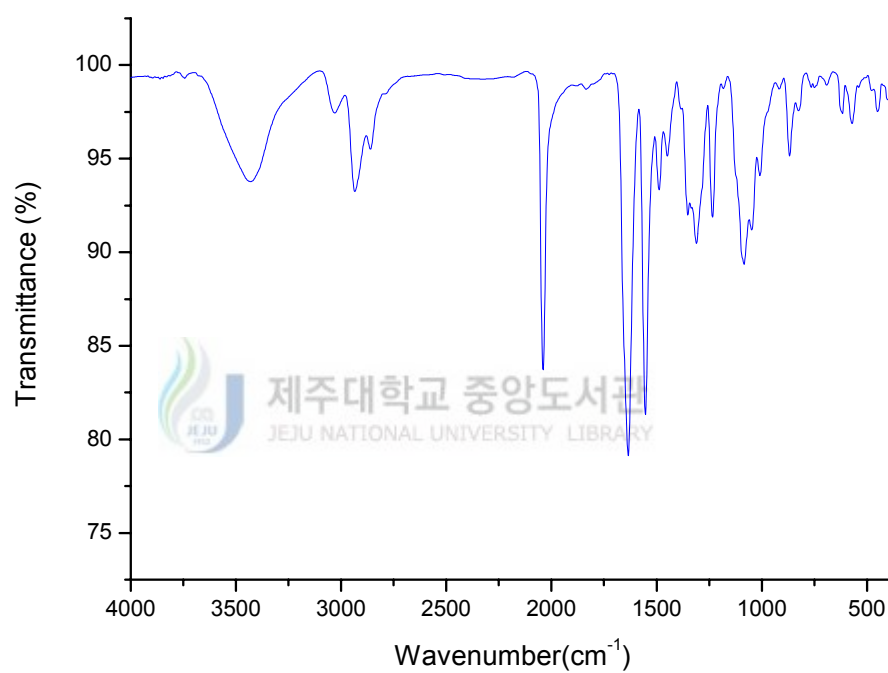
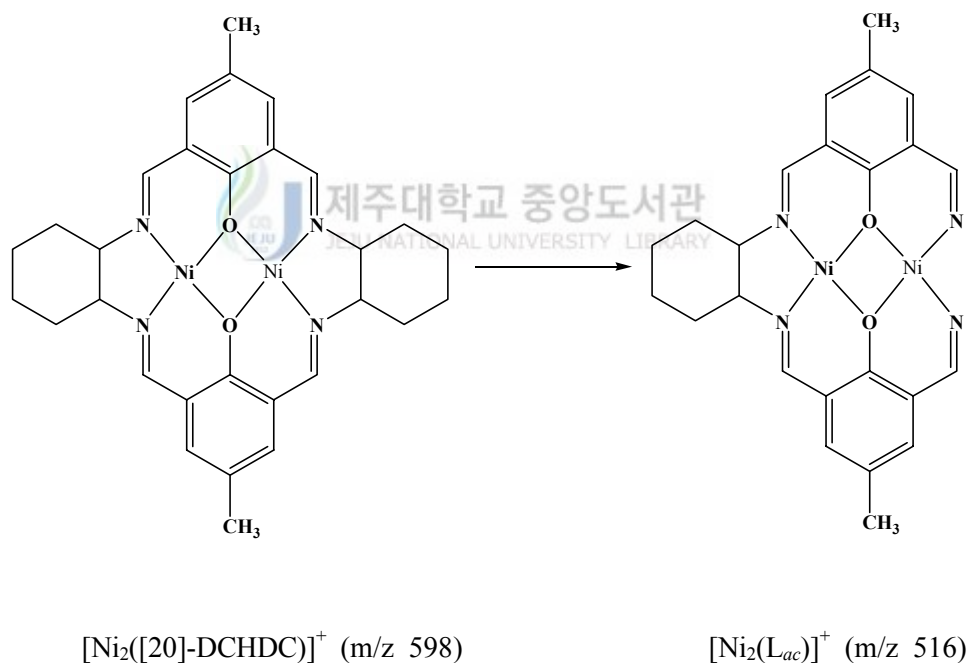


Figure 8. FT-IR spectrum of [Ni(H₂[20]-DCHDC)(NCS)₂] complex.

2. FAB-mass spectra of the complexes

The FAB mass spectra of the Ni(II) complexes were shown in Figure 9~16, and summarized at Table 11. The molecular ion loses the exocyclic ligands resulting in the formation of the fragment $[\text{Ni}_2([\text{20}]\text{-DCHDC})]^+$. All these species are well observed in the FAB mass spectra at m/z 598 region. α -cleavage peaks of one cyclohexane from the $[\text{Ni}_2([\text{20}]\text{-DCHDC})]^+$ ion in the formation of the fragment $[\text{Ni}_2(\text{L}_{ac})]^+$ are observed at m/z 516 region.



Removal peaks of one nickel ion from the $[\text{Ni}_2([\text{20}]\text{-DCHDC})]^+$ ion in the formation of the fragment $[\text{Ni}([\text{20}]\text{-DCHDC})]^+$ is observed at m/z 540. The

FAB mass spectra of the complexes contain peaks corresponding to the $[\text{H}_2[20]\text{-DCHDC}]^+$ fragment ion at m/z 484 region. This indicates that the species $[\text{Ni}_2([20]\text{-DCHDC})]^+$ undergoes demetallation to give the tetraazadioxa macrocycle $\text{H}_2[20]\text{-DCHDC}$ under FAB conditions. These peaks are associated with peaks of mass one or two greater or less, which are attributed to protonated/deprotonated forms. This also accounts for the slight ambiguities in making assignments. Removal peaks of one exocyclic ligand resulting in the formation of the fragment $[\text{Ni}_2([20]\text{-DCHDC})(\text{L}_a)]^+$ ($\text{L}_a = \text{Cl}^-$, ClO_4^- , NCS^- , N_3^- and NO_2^-) are observed at m/z 635.1, 699.4, 662.4, 647.4 and 644.1 respectively.

The FAB mass spectra of $[\text{Ni}(\text{H}_2[20]\text{-DCHDC})(\text{ClO}_4)_2]$ complexes contain peaks corresponding to the $[\text{Ni}(\text{H}_2[20]\text{-DCHDC})(\text{ClO}_4)]^+$ fragment ion at m/z 740.2 region. Removal peaks of one perchlorate ion from the $[\text{Ni}(\text{H}_2[20]\text{-DCHDC})(\text{ClO}_4)_2 \cdot 2\text{H}_2\text{O}]$ complexes in the formation of the fragment $[\text{Ni}(\text{H}_2[20]\text{-DCHDC})(\text{ClO}_4)]^+$ is observed at m/z 641.2 region.

Table 11. FAB-mass spectra for the Ni(II) complexes of phenol-based macrocyclic ligand (H₂[20]-DCHDC)

complex	m/z	Assignments	
[Ni ₂ ([20]-DCHDC)]Cl ₂	459.2	[Ni(L _{ac})+H] ⁺	458.1
	484.6	[H ₂ ([20]-DCHDC)] ⁺	484.3
	516.1	[Ni ₂ (L _{ac})] ⁺	516.1
	541.3	[Ni([20]-DCHDC)+H] ⁺	540.2
	598.1	[Ni ₂ ([20]-DCHDC)] ⁺	598.1
	635.1	[Ni ₂ ([20]-DCHDC)(Cl)+2H] ⁺	633.1
[Ni ₂ ([20]-DCHDC)](ClO ₄) ₂	459.2	[Ni(L _{ac})+H] ⁺	458.1
	516.1	[Ni ₂ (L _{ac})] ⁺	516.1
	541.3	[Ni([20]-DCHDC)+H] ⁺	540.2
	598.1	[Ni ₂ ([20]-DCHDC)] ⁺	598.1
	699.4	[[Ni ₂ ([20]-DCHDC)(ClO ₄)+2H] ⁺	697.1
[Ni ₂ ([20]-DCHDC)(NCS) ₂]	541.2	[Ni([20]-DCHDC)+H] ⁺	540.2
	598.1	[Ni ₂ ([20]-DCHDC)] ⁺	589.1
	662.4	[Ni ₂ ([20]-DCHDC)(NCS)+6H] ⁺	656.1
[Ni ₂ ([20]-DCHDC)(N ₃) ₂]	516.1	[Ni ₂ (L _{ac})-H] ⁺	516.1
	541.2	[Ni([20]-DCHDC)+H] ⁺	540.2
	598.1	[Ni ₂ ([20]-DCHDC)] ⁺	598.1
	647.4	[Ni ₂ ([20]-DCHDC)(N ₃)+7H] ⁺	640.1
[Ni ₂ ([20]-DCHDC)(μ-ONO)]NO ₂ · 1.5H ₂ O	516.1	[Ni ₂ (L _{ac})] ⁺	516.1
	541.2	[Ni([20]-DCHDC)+H] ⁺	540.2
	598.1	[Ni ₂ ([20]-DCHDC)] ⁺	598.1
	644.1	[Ni ₂ ([20]-DCHDC)(NO ₂)] ⁺	644.1
[Ni ₂ ([20]-DCHDC)I ₂]	541.2	[Ni([20]-DCHDC+H)] ⁺	540.2
	598.1	[Ni ₂ ([20]-DCHDC)] ⁺	598.1
[Ni(H ₂ [20]-DCHDC)](ClO ₄) ₂ ·2H ₂ O	541.2	[Ni(H ₂ [20]-DCHDC)-H] ⁺	542.2
	641.2	[[Ni(H ₂ [20]-DCHDC)(ClO ₄)] ⁺	641.2
	741.4	[Ni(H ₂ [20]-DCHDC)(ClO ₄) ₂ +H] ⁺	740.1
[Ni(H ₂ [20]-DCHDC)(NCS) ₂] · 3H ₂ O	541.2	[Ni(H ₂ [20]-DCHDC)-H] ⁺	542.2
	598.6	[[Ni(H ₂ [20]-DCHDC)NCS-H] ⁺	600.2

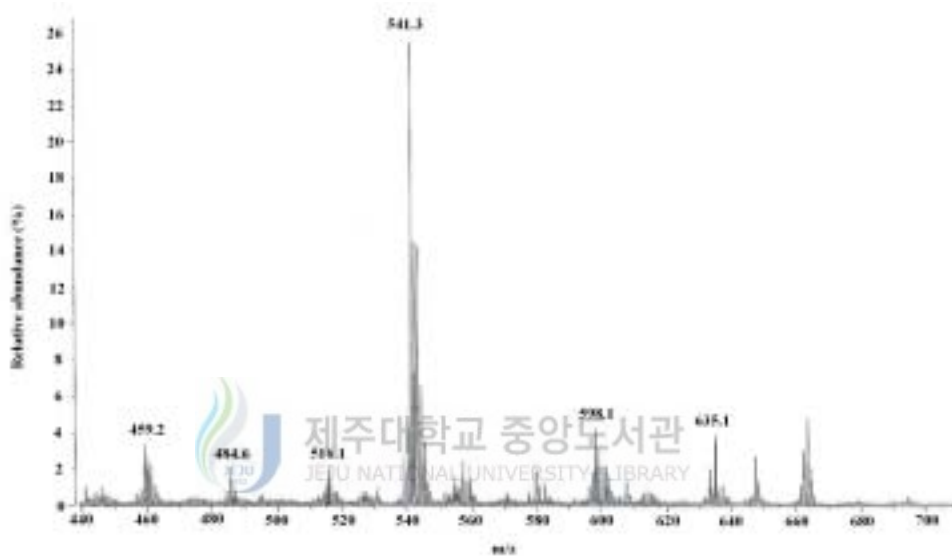


Figure 9. FAB mass spectrum of the $[\text{Ni}_2([\text{20}]\text{-DCHDC})]\text{Cl}_2$.

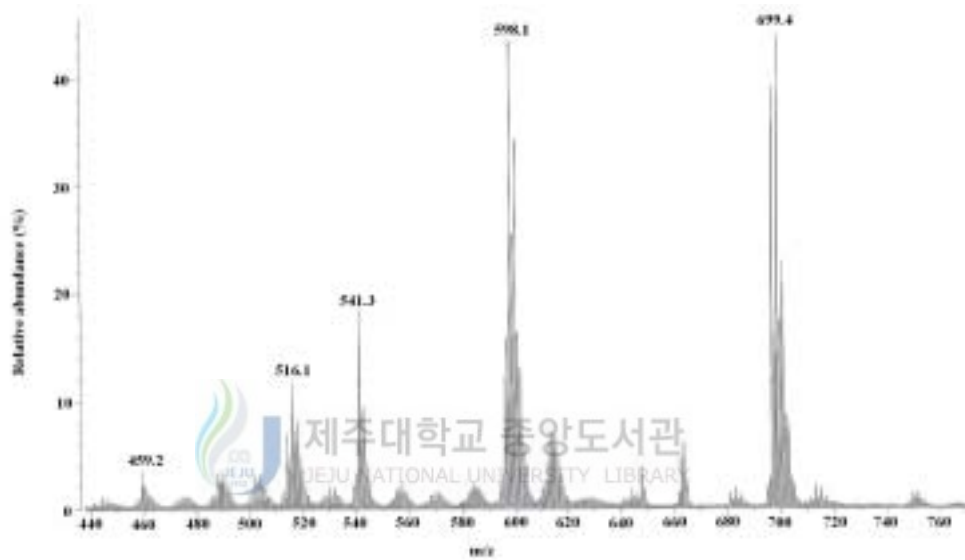


Figure 10. FAB mass spectrum of the $[\text{Ni}_2([\text{20}]\text{-DCHDC})](\text{ClO}_4)_2$.

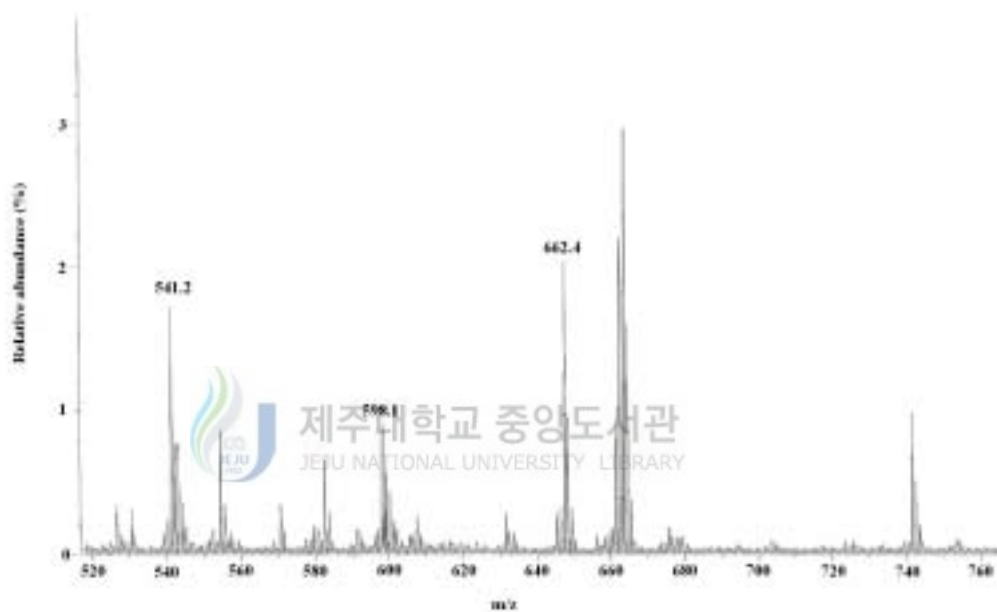


Figure 11. FAB mass spectrum of the $[\text{Ni}_2([\text{20}]\text{-DCHDC})(\text{NCS})_2]$.

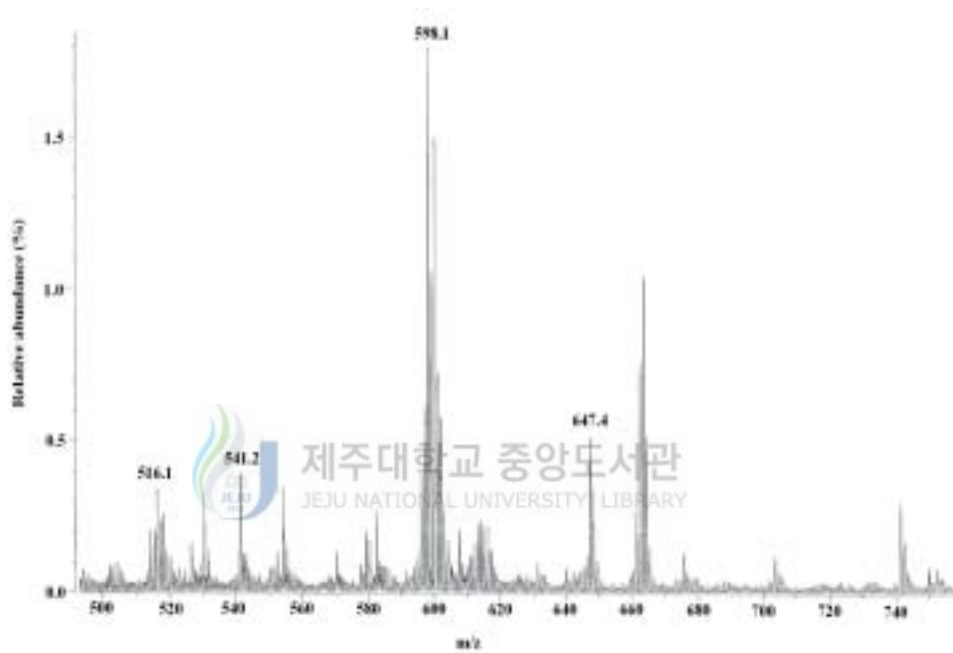


Figure 12. FAB mass spectrum of the $[\text{Ni}_2([\text{20}]\text{-DCHDC})(\text{N}_3)_2]$.

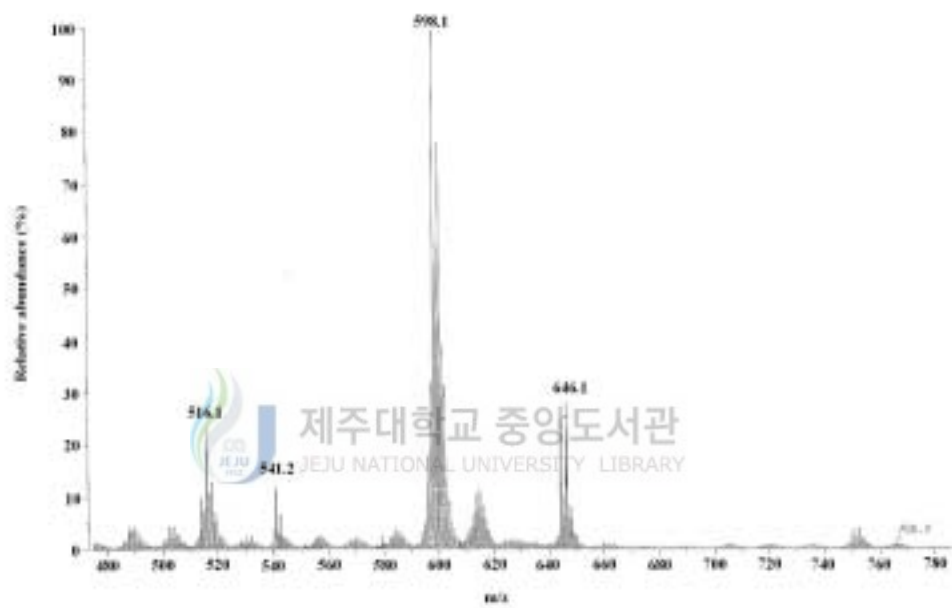


Figure 13. FAB mass spectrum of the $[\text{Ni}_2([\text{20}]\text{-DCHDC})(\mu\text{-ONO})]\text{NO}_2 \cdot 1.5\text{H}_2\text{O}$.

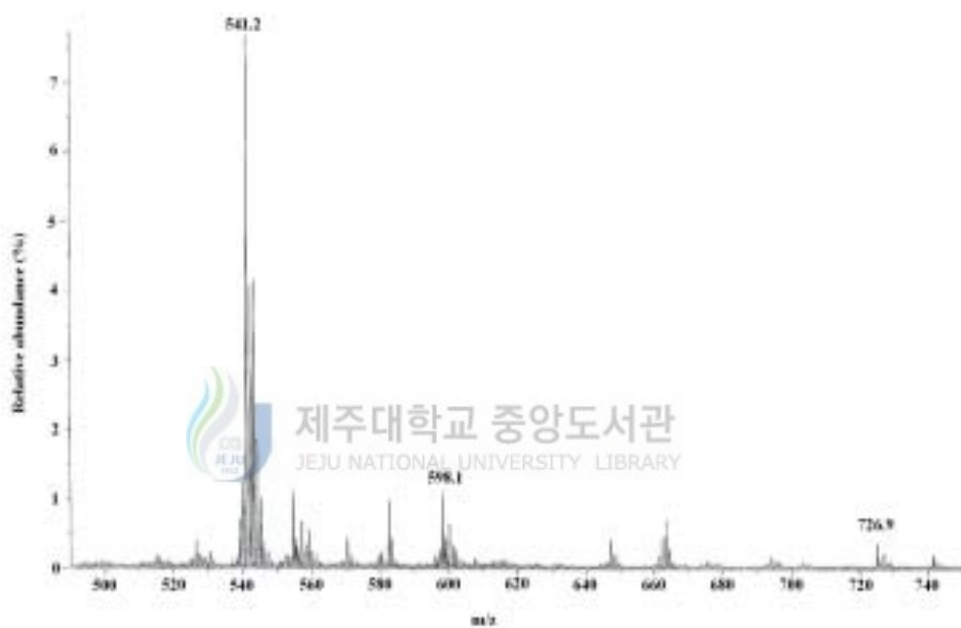


Figure 14. FAB mass spectrum of the $[\text{Ni}_2([\text{20}]\text{-DCHDC})\text{I}_2]$.

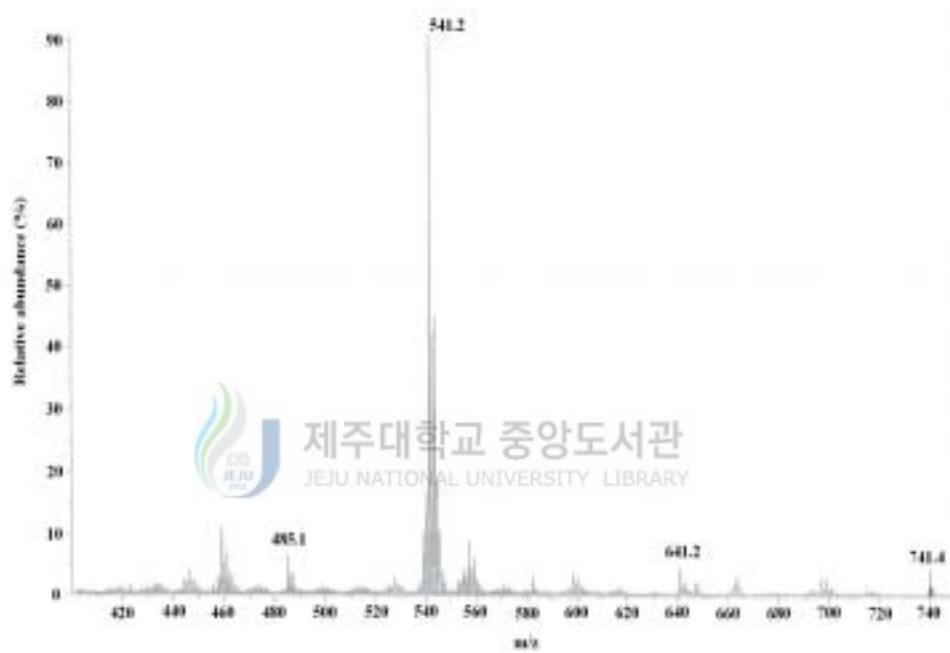


Figure 15. FAB mass spectrum of the $[\text{Ni}(\text{H}_2[20]\text{-DCHDC})](\text{ClO}_4)_2 \cdot 2\text{H}_2\text{O}$.

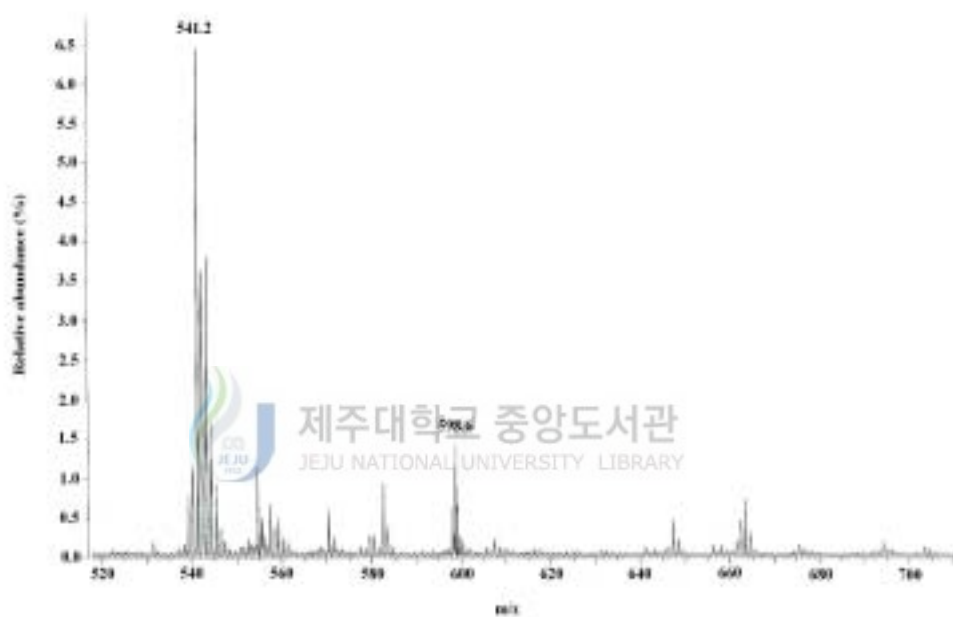


Figure 16. FAB mass spectrum of the $[\text{Ni}(\text{H}_2[20]\text{-DCHDC})(\text{NCS})_2] \cdot 3\text{H}_2\text{O}$.

3. Electronic absorption spectrum of Ni(II) complexes

The electronic absorption spectra of Ni(II) complexes at room temperature were represented in Figure 17~23 and summarized Table 12. The electronic absorption spectrum of this solution is typical of six-coordinate nickel(II) complex indicating that species existing in solution is $[\text{Ni}_2([\text{20}]\text{-DCHDC})\text{-(OH}_2)_2]^{2+}$. Much weaker bands are found at lower energy, associated with *d-d* transitions. However, strong absorptions at 300 - 450 nm are clearly associated with ligand to metal charge transfer transitions, which reflect the presence of highly delocalized π macrocyclic framework. The ground state of d^8 in an octahedral coordination is ${}^3\text{A}_{2g}$. Two *d-d* bands observed for the complex at $13,717\text{ cm}^{-1}$ ($\epsilon = 8.4\text{ M}^{-1}\text{cm}^{-1}$), $18,051\text{ cm}^{-1}$ ($\epsilon = 19.2\text{ M}^{-1}\text{cm}^{-1}$) can be attributed in an octahedral model to the transition. Thus, these bands may be assigned to the spin allowed transitions ${}^3\text{A}_{2g} \rightarrow {}^3\text{T}_{2g}$ (F) and ${}^3\text{A}_{2g} \rightarrow {}^3\text{T}_{1g}$ (F), respectively. ${}^3\text{A}_{2g} \rightarrow {}^3\text{T}_{1g}$ (P) transition is not separated by the transfer effect to visible range of charge transfer transitions and absorptions of macrocycle ligand.³⁰

Table 12. Electronic spectral data (λ_{max} ; nm, ϵ ; $\text{M}^{-1} \text{cm}^{-1}$) for the Ni(II) macrocyclic complexes

Complexes	medium	λ_{max} (ϵ)	medium	λ_{max}
$[\text{Ni}_2([20]\text{-DCHDC})\text{Cl}_2]$	MeOH	330sh (7944), 401(8744)	solid	450, 622
$[\text{Ni}_2([20]\text{-DCHDC})](\text{ClO}_4)_2$	DMSO	389 (10333)	solid	380, 494sh, 591
$[\text{Ni}_2([20]\text{-DCHDC})(\text{NCS})_2]$	DMSO	392 (10690), 419sh (10212)	solid	397sh, 525, 598
$[\text{Ni}_2([20]\text{-DCHDC})(\text{N}_3)_2]$	DMSO	389 (14181)	solid	463, 546sh,
$[\text{Ni}_2([20]\text{-DCHDC})(\mu\text{-ONO})]\text{NO}_2 \cdot 1.5\text{H}_2\text{O}$	DMSO	386 (12640)	solid	446, 544
$[\text{Ni}_2([20]\text{-DCHDC})\text{I}_2]$	DMSO	393 (9588), 420sh (9005)	solid	407sh, 470, 597sh
$[\text{Ni}(\text{H}_2[20]\text{-DCHDC})](\text{ClO}_4)_2 \cdot 2\text{H}_2\text{O}$	DMSO	418 (13120)	solid	382sh, 480
$[\text{Ni}(\text{H}_2[20]\text{-DCHDC})(\text{NCS})_2] \cdot 3\text{H}_2\text{O}$	DMSO	332sh (10969), 420 (13882)	solid	495, 603sh

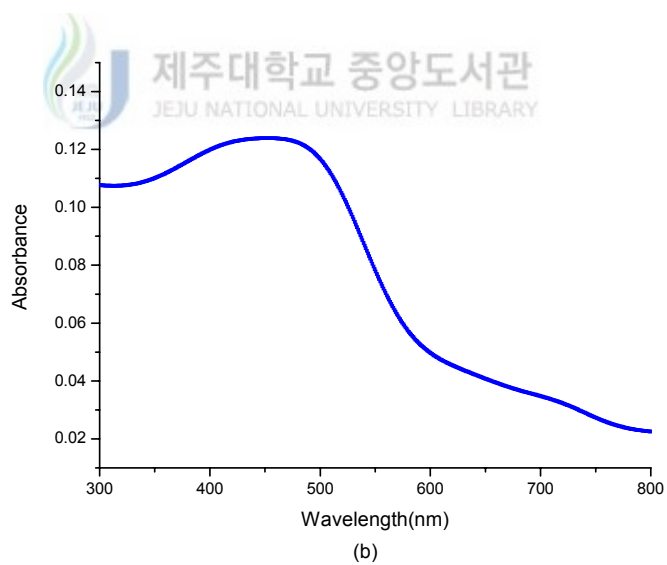
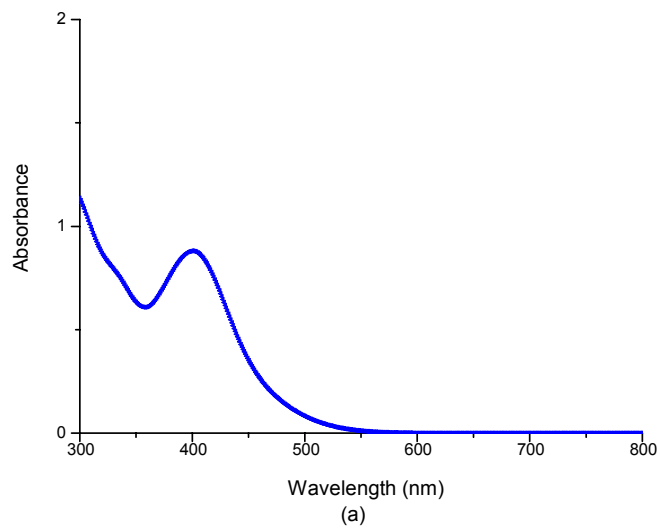


Figure 17. Electronic absorption spectrum of $[\text{Ni}_2([\text{20}]\text{-DCHDC})\text{Cl}_2$ in (a) methanol (1.0×10^{-4} M) and (b) solid (BaSO_4).

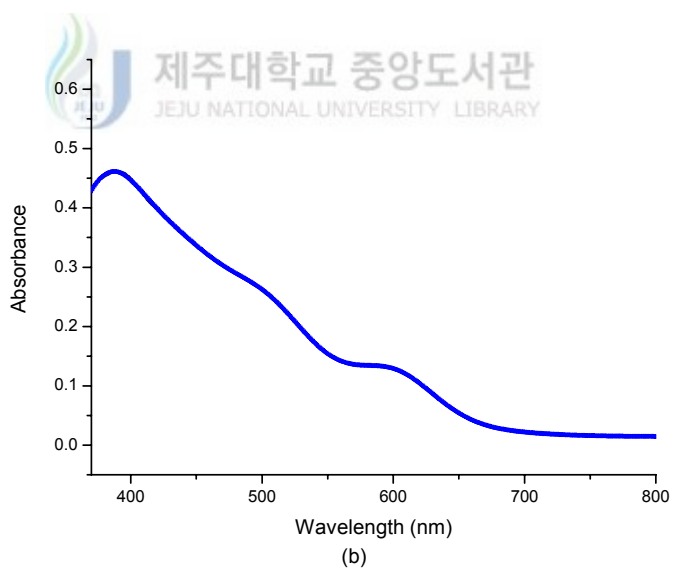
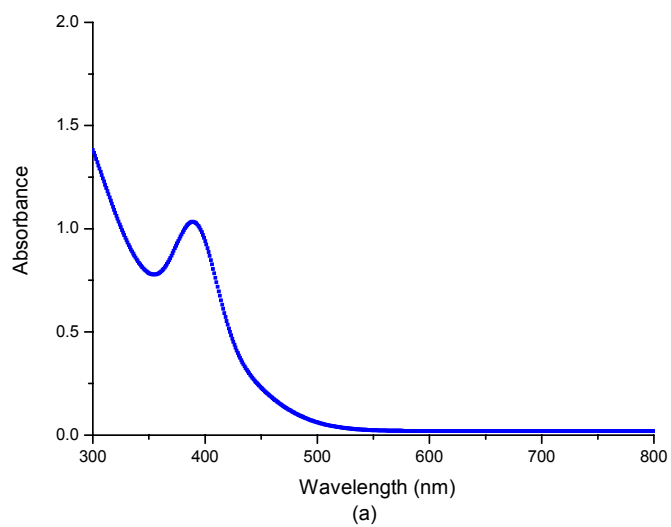


Figure 18. Electronic absorption spectrum of $[\text{Ni}_2([\text{20}]\text{-DCHDC})](\text{ClO}_4)_2$ in (a) DMSO (1.0×10^{-4} M) and (b) solid (BaSO_4).

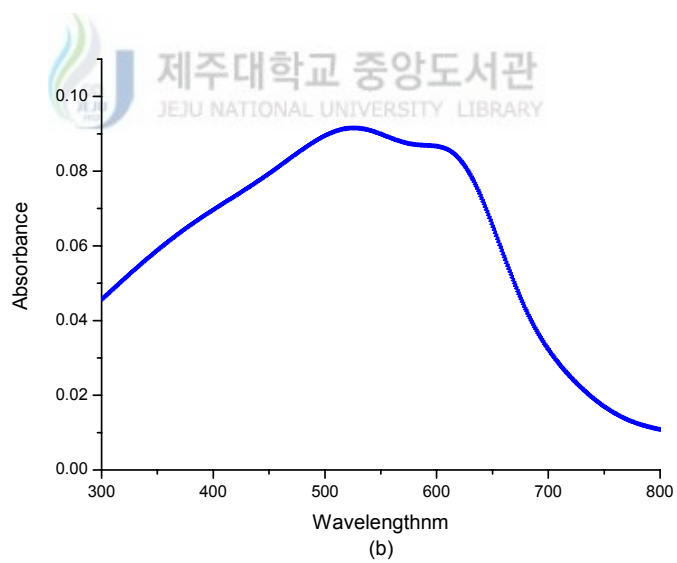
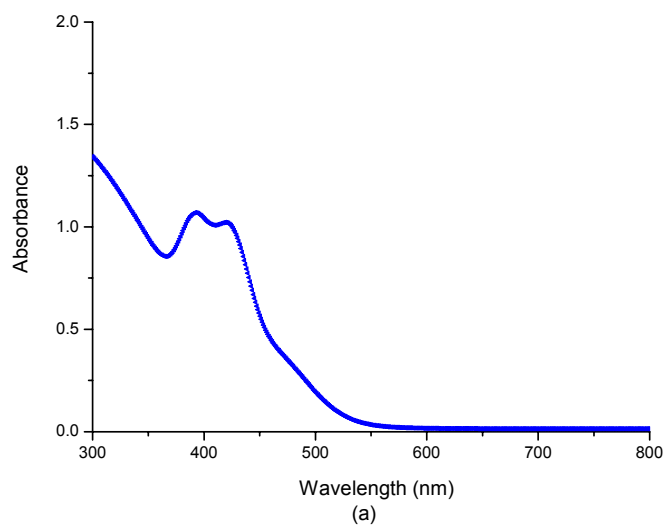


Figure 19. Electronic absorption spectrum of $[\text{Ni}_2([\text{20}]\text{-DCHDC})(\text{NCS})_2]$ in (a) DMSO (1.0×10^{-4} M) and (b) solid (BaSO_4).

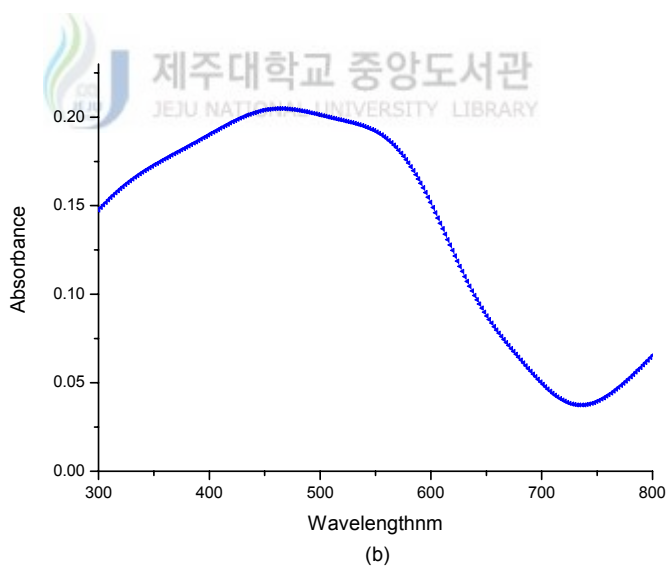
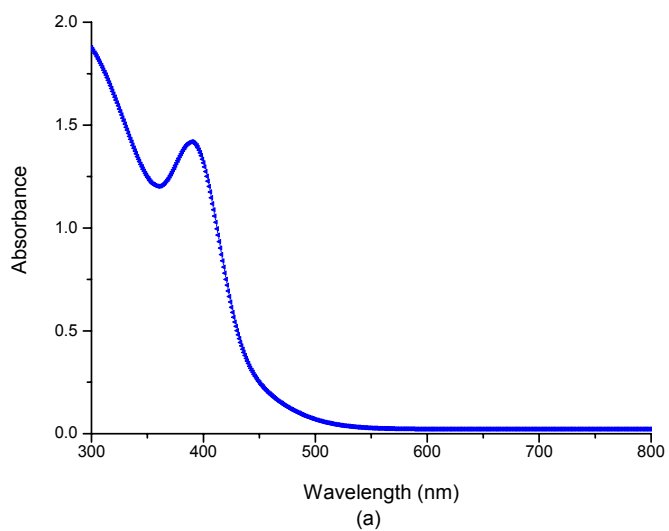


Figure 20. Electronic absorption spectrum of $[\text{Ni}_2([\text{20}]\text{-DCHDC})(\text{N}_3)_2]$ in (a) DMSO (1.0×10^{-4} M) and (b) solid (BaSO_4).

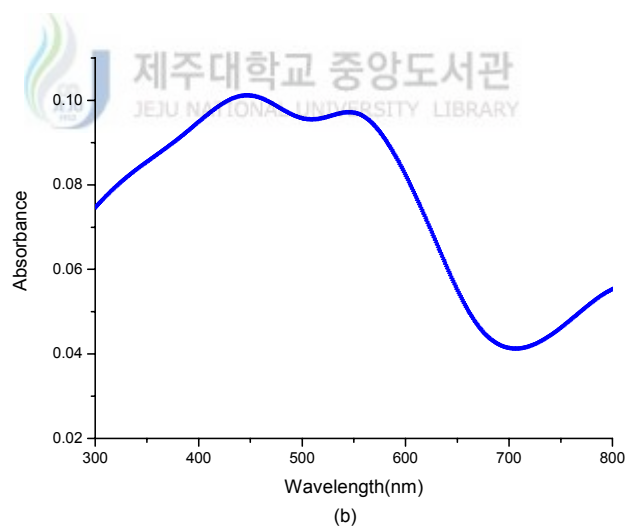
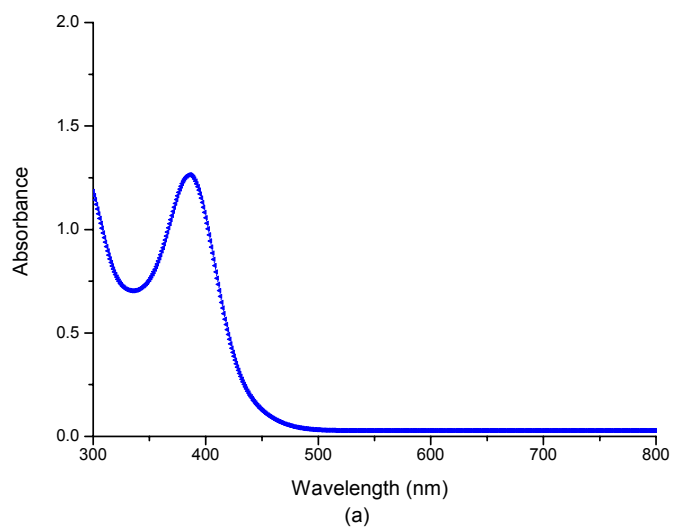


Figure 21. Electronic absorption spectrum of $[\text{Ni}_2([\text{20}]\text{-DCHDC})(\mu\text{-ONO})]\text{NO}_2 \cdot 1.5\text{H}_2\text{O}$ in (a) DMSO (1.0×10^{-4} M) and (b) solid (BaSO_4)

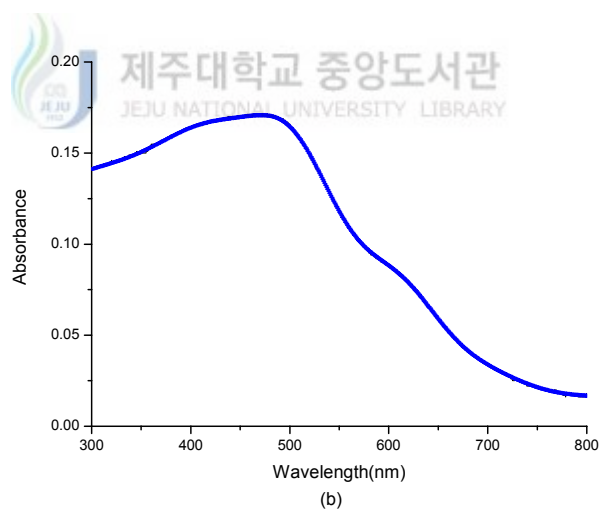
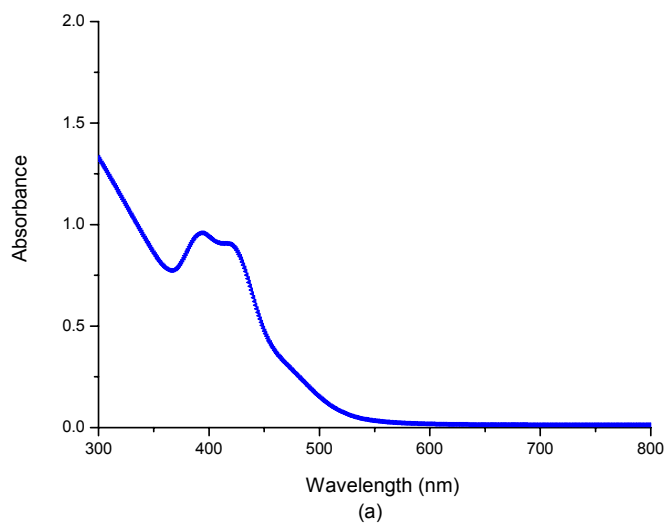


Figure 22. Electronic absorption spectrum of $[\text{Ni}_2([\text{20}]\text{-DCHDC})\text{I}_2]$ in (a) DMSO (1.0×10^{-4} M) and (b) solid (BaSO_4).

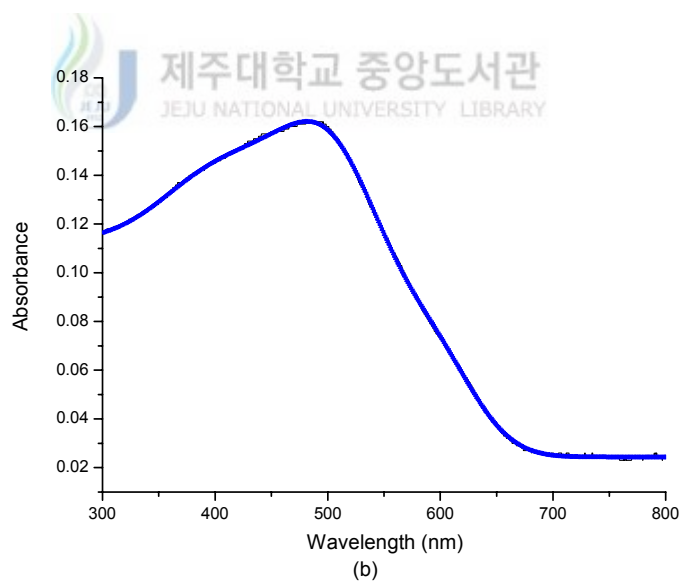
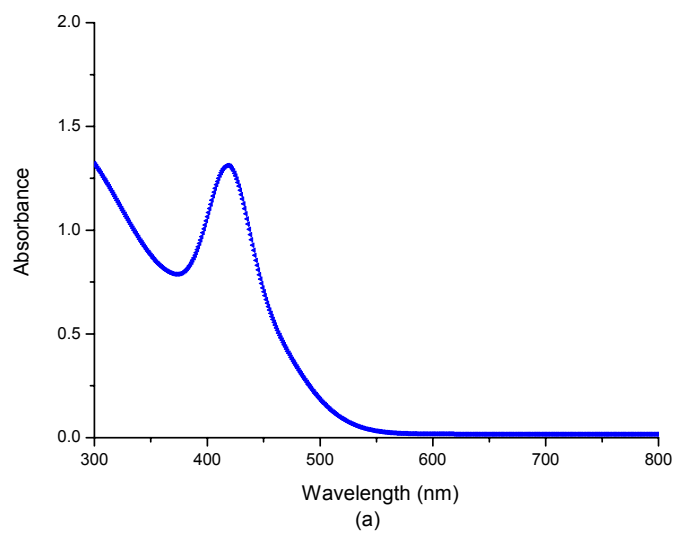


Figure 23. Electronic absorption spectrum of $[\text{Ni}(\text{H}_2[20]\text{-DCHDC})](\text{ClO}_4)_2 \cdot 2\text{H}_2\text{O}$ in (a) DMSO (1.0×10^{-4} M) and (b) solid (BaSO_4).

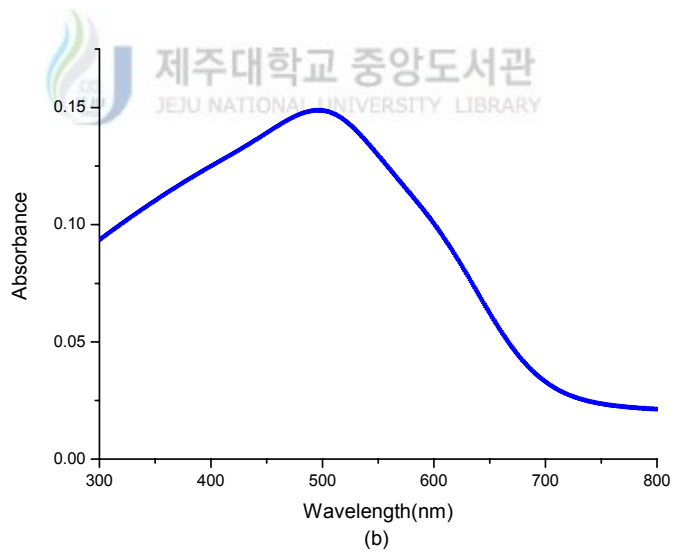
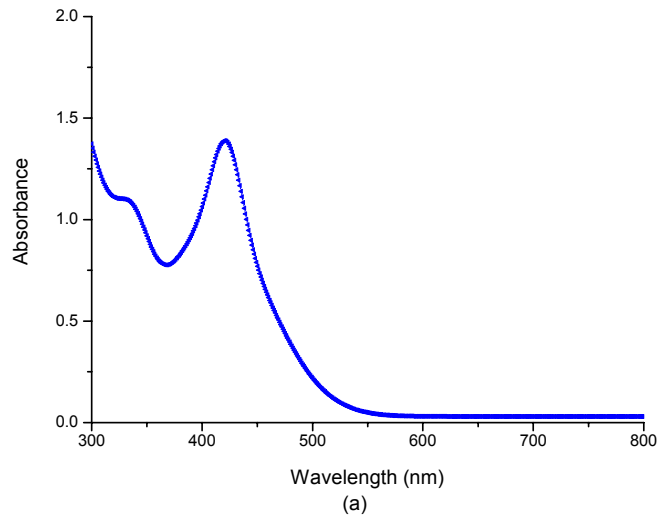


Figure 24. Electronic absorption spectrum of $[\text{Ni}(\text{H}_2[20]\text{-DCHDC})(\text{NCS})_2] \cdot 3\text{H}_2\text{O}$ in (a) DMSO (2.5×10^{-4} M) and (b) solid (BaSO_4).

4. Crystal Structures of Complexes

1) $[\text{Ni}_2([\text{20}]\text{-DCHDC})](\text{ClO}_4)_2 \cdot 2\text{CH}_3\text{CN}$

Crystals of $[\text{Ni}_2([\text{20}]\text{-DCHDC})](\text{ClO}_4)_2 \cdot 2\text{CH}_3\text{CN}$ suitable for X-ray diffraction study were obtained by slow evaporation of acetonitrile solution of the $[\text{Ni}_2([\text{20}]\text{-DCHDC})](\text{ClO}_4)_2$ complex.

Two formula units comprise the unit cell with half of the binuclear complex in the asymmetric unit. An ORTEP drawing of asymmetric unit and core structure (top view) for the complex are given in Figure 24 and 25, respectively.



Figure 25. Structural representation of asymmetric unit of $[\text{Ni}_2([\text{20}]\text{-DCHDC})](\text{ClO}_4)_2 \cdot 2\text{CH}_3\text{CN}$ complex.

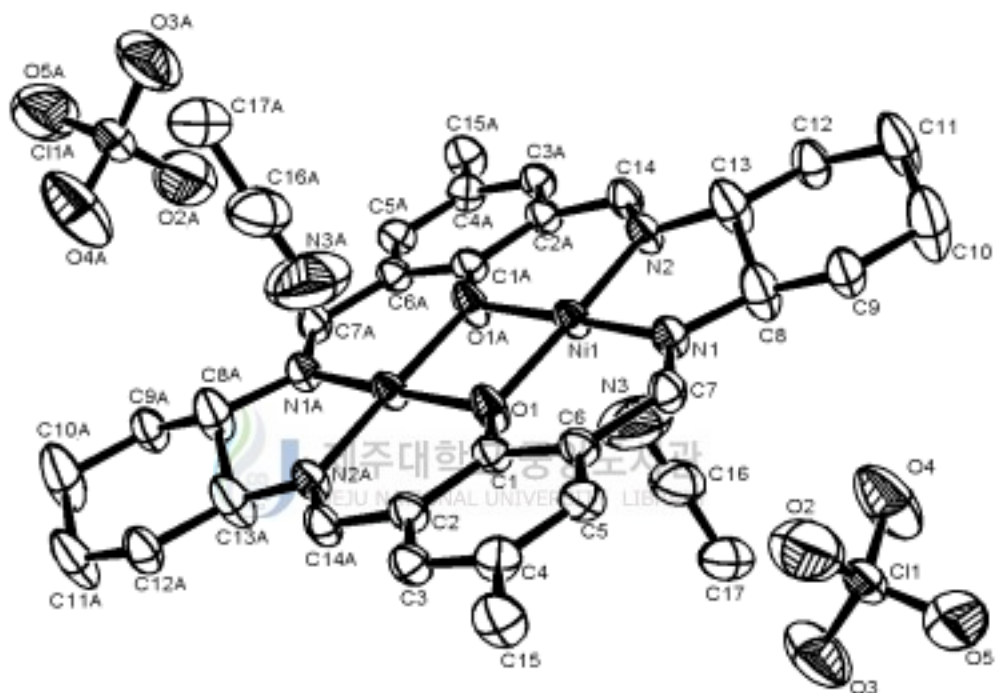
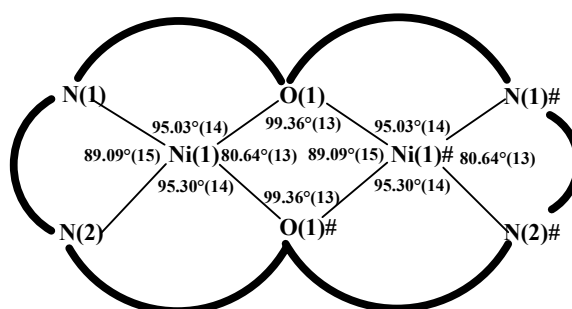


Figure 26. An ORTEP view of core structure (top view) for the binuclear complex showing 50% probability thermal ellipsoids and labels for non-H atoms.

The crystal structure of this complex is composed of binuclear cation of the indicated formula and noninteracting perchlorate anions. These results are backed up by the molar conductivity ($\Lambda_M = 311 \text{ ohm}^{-1}\text{cm}^2\text{mol}^{-1}$) which agreed with assignment of the structure as $[\text{Ni}_2([\text{20}]\text{-DCHDC})](\text{ClO}_4)_2$.



The binuclear cation, $[\text{Ni}_2([\text{20}]\text{-DCHDC})]^{2+}$ shows two square-planar environment, where the nickel(II) ions are coordinated by basal planes (N_2O_2), respectively. The binuclear core structures are centrosymmetric with each Ni(II) ion in the $\text{N}(\text{imine})_2\text{O}_2$ sites being four-coordinate by square-planar geometry of interactions with two nitrogen and two oxygen atoms of the binucleating ligand [20]-DCHDC. The macrocyclic complex adopts an essentially flat structure with the two square-plane nickel centers bridged by the two phenoxide oxygen atoms; the dihedral angle between the plane defined by N(1), O(1), and O(1)# and the plane defined by Ni(1)#, O(1), and O(1)# is 178.01° . The sum of angles at the nickel basal planes (NiN_2O_2) is almost exactly 360° (359.79°), indicating no plane distortion.

The angle of C(1)-O(1)-O(1)# is 166.55° . This value is smaller than the ideal value of 180° , indicating that the two phenol mean planes are not able to flat. The interatomic $\text{Ni}(1)\cdots\text{Ni}(1)\#$ separation is $2.8078(10) \text{ \AA}$. The in-plane Ni-to-donor distances range from $1.827(3)$ to $1.842(3) \text{ \AA}$. The

perchlorate ions and acetonitrile molecules occupy lattice sites. The Ni···N(3) (acetonitrile) separation is 3.256 Å. The Ni···O(16) (perchlorate) separation is 4.759 Å.

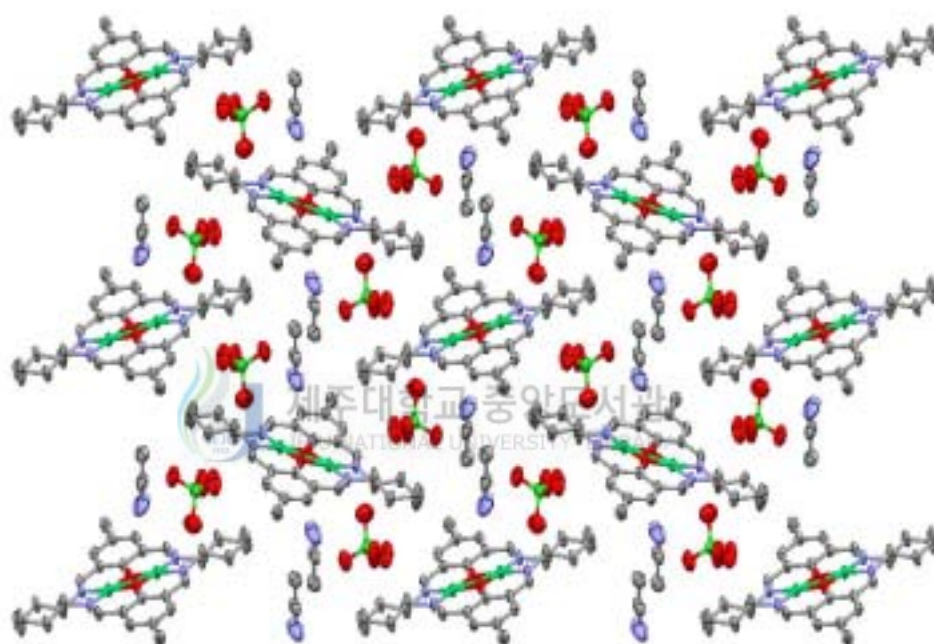


Figure 27. The molecular packing diagram of $[\text{Ni}_2([\text{20}]\text{-DCHDC})](\text{ClO}_4)_2 \cdot 2\text{CH}_3\text{CN}$.

Table 13. Bond lengths (Å) for $[\text{Ni}_2([\text{20}]\text{-DCHDC})](\text{ClO}_4)_2 \cdot 2\text{CH}_3\text{CN}$ complex

Ni(1)-N(1)	1.827(3)	C(4)-C(15)	1.516(6)
Ni(1)-N(2)	1.828(3)	C(5)-C(6)	1.403(5)
Ni(1)-O(1)#1	1.841(3)	C(6)-C(7)	1.453(6)
Ni(1)-O(1)	1.842(3)	C(8)-C(13)	1.461(7)
Ni(1)-Ni(1)#1	2.8078(10)	C(8)-C(9)	1.517(6)
O(1)-C(1)	1.324(5)	C(9)-C(10)	1.514(7)
O(1)-Ni(1)#1	1.841(3)	C(10)-C(11)	1.446(8)
N(1)-C(7)	1.279(5)	C(11)-C(12)	1.519(7)
N(1)-C(8)	1.484(6)	C(12)-C(13)	1.526(6)
N(2)-C(14)	1.289(5)	C(14)-C(2)#1	1.452(6)
N(2)-C(13)	1.495(6)	Cl(1)-O(4)	1.405(5)
C(1)-C(6)	1.411(6)	Cl(1)-O(3)	1.407(5)
C(1)-C(2)	1.414(5)	Cl(1)-O(2)	1.424(6)
C(2)-C(3)	1.399(5)	Cl(1)-O(5)	1.447(5)
C(2)-C(14)#1	1.452(6)	N(3)-C(16)	1.140(9)
C(3)-C(4)	1.393(6)	C(16)-C(17)	1.424(9)
C(4)-C(5)	1.375(6)		

Symmetry transformations used to generate equivalent atoms:

#1; $-x+1, y, z$.

Table 14. Angles [°] for [Ni₂([20]-DCHDC)](ClO₄)₂ · 2CH₃CN complex

N(1)-Ni(1)-N(2)	89.09(15)	C(5)-C(4)-C(3)	118.4(4)
N(1)-Ni(1)-O(1)#1	174.76(14)	C(5)-C(4)-C(15)	120.9(4)
N(2)-Ni(1)-O(1)#1	95.30(14)	C(3)-C(4)-C(15)	120.7(4)
N(1)-Ni(1)-O(1)	95.03(14)	C(4)-C(5)-C(6)	122.2(4)
N(2)-Ni(1)-O(1)	175.76(14)	C(5)-C(6)-C(1)	118.8(4)
O(1)#1-Ni(1)-O(1)	80.64(13)	C(5)-C(6)-C(7)	118.6(4)
N(1)-Ni(1)-Ni(1)#1	135.27(11)	C(1)-C(6)-C(7)	122.6(3)
N(2)-Ni(1)-Ni(1)#1	135.61(11)	N(1)-C(7)-C(6)	125.7(4)
O(1)#1-Ni(1)-Ni(1)#1	40.33(8)	C(13)-C(8)-N(1)	107.6(4)
O(1)-Ni(1)-Ni(1)#1	40.31(9)	C(13)-C(8)-C(9)	113.3(5)
C(1)-O(1)-Ni(1)#1	128.8(3)	N(1)-C(8)-C(9)	116.8(4)
C(1)-O(1)-Ni(1)	129.2(3)	C(10)-C(9)-C(8)	109.2(4)
Ni(1)#1-O(1)-Ni(1)	99.36(13)	C(11)-C(10)-C(9)	115.8(5)
C(7)-N(1)-C(8)	123.5(4)	C(10)-C(11)-C(12)	116.3(5)
C(7)-N(1)-Ni(1)	125.8(3)	C(11)-C(12)-C(13)	108.9(4)
C(8)-N(1)-Ni(1)	110.4(3)	C(8)-C(13)-N(2)	107.4(4)
C(14)-N(2)-C(13)	124.1(4)	C(8)-C(13)-C(12)	113.6(5)
C(14)-N(2)-Ni(1)	125.5(3)	N(2)-C(13)-C(12)	116.7(4)
C(13)-N(2)-Ni(1)	110.3(3)	N(2)-C(14)-C(2)#1	125.3(4)
O(1)-C(1)-C(6)	119.9(3)	O(4)-Cl(1)-O(3)	114.0(3)
O(1)-C(1)-C(2)	120.2(4)	O(4)-Cl(1)-O(2)	110.0(4)
C(6)-C(1)-C(2)	119.9(3)	O(3)-Cl(1)-O(2)	109.8(3)
C(3)-C(2)-C(1)	118.5(4)	O(4)-Cl(1)-O(5)	108.9(3)
C(3)-C(2)-C(14)#1	118.5(4)	O(3)-Cl(1)-O(5)	109.7(3)
C(1)-C(2)-C(14)#1	122.9(4)	O(2)-Cl(1)-O(5)	104.1(4)
C(4)-C(3)-C(2)	122.1(4)	N(3)-C(16)-C(17)	177.6(8)

Symmetry transformations used to generate equivalent atoms:

#1 -x+1, y, z.

2) $[\text{Ni}(\text{H}_2[20]\text{-DCHDC})](\text{ClO}_4)_2$

Suitable crystals of $[\text{Ni}(\text{H}_2[20]\text{-DCHDC})](\text{ClO}_4)_2$ were obtained by slow evaporation of methanol solutions of $[\text{Ni}(\text{H}_2[20]\text{-DCHDC})](\text{ClO}_4)_2 \cdot 2\text{H}_2\text{O}$ complex at atmospheric pressure.

Two formula units comprise the unit cell with half of the mononuclear complex in the asymmetric unit. An ORTEP drawing of asymmetric unit and core structure (top view) for the complex are given in Figure 27 and 28, respectively.

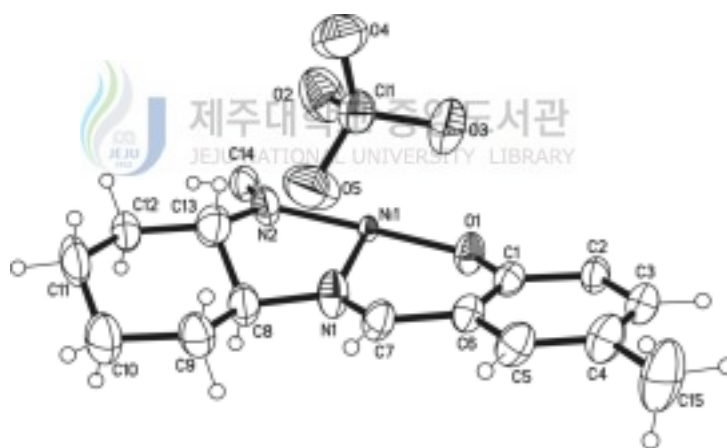


Figure 28. Structural representation of asymmetric unit of $[\text{Ni}(\text{H}_2[20]\text{-DCHDC})](\text{ClO}_4)_2$ complex.

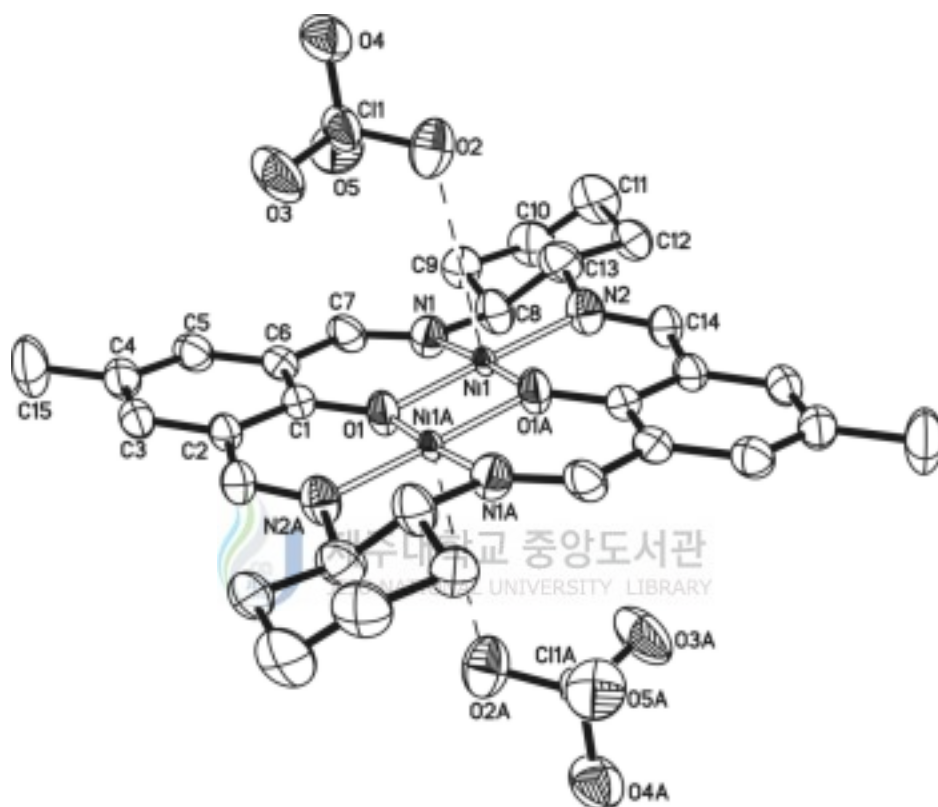


Figure 29. An ORTEP view of core structure (top view) for the mononuclear complex showing 50% probability thermal ellipsoids and labels for non-H atoms.

The crystal structure of this complex is composed of mononuclear cation of the indicated formula and noninteracting perchloride anions. These results are backed up by the molar conductivity ($\Lambda_M = 322 \text{ ohm}^{-1}\text{cm}^2\text{mol}^{-1}$) which agreed with assignment of the structure as $[\text{Ni}(\text{H}_2[20]\text{-DCHDC})](\text{ClO}_4)_2$. The mononuclear cation, $[\text{Ni}(\text{H}_2[20]\text{-DCHDC})]^{2+}$ shows two square-plane environment, where the nickel(II) ions are coordinated by basal planes (NiN_2O_2), one side. The occupancy of central metal Ni(II) is 0.5.

The geometry about Ni(1) in the N_2O_2 site is a square-planar environment, and other N_2O_2 site is able to vacant. The macrocyclic complex adopts an essentially flat structure with the square-planar nickel center bridged by the two phenoxide oxygen atoms the dihedral angle between the plane defined by N(1A), O(1), and O(1A) and the plane defined by Ni(1), O(1), and O(1A) is 179.15° . The sum of angles at the nickel basal planes (NiN_2O_2) is almost exactly $360^\circ(359.97^\circ)$, indicating no plane distortion. The angle of C(1)-O(1)-O(1A) is 162.80° . This value is smaller than the ideal value of 180° , indicating that the two phenol mean planes are not able to flat. The in-plane Ni-to-donor distances range from 1.743(4) to 1.907(6) Å. The perchlorate ions occupy lattice sites. The Ni(1)⋯O(2) (perchlorate) separation is 3.453(6) Å.

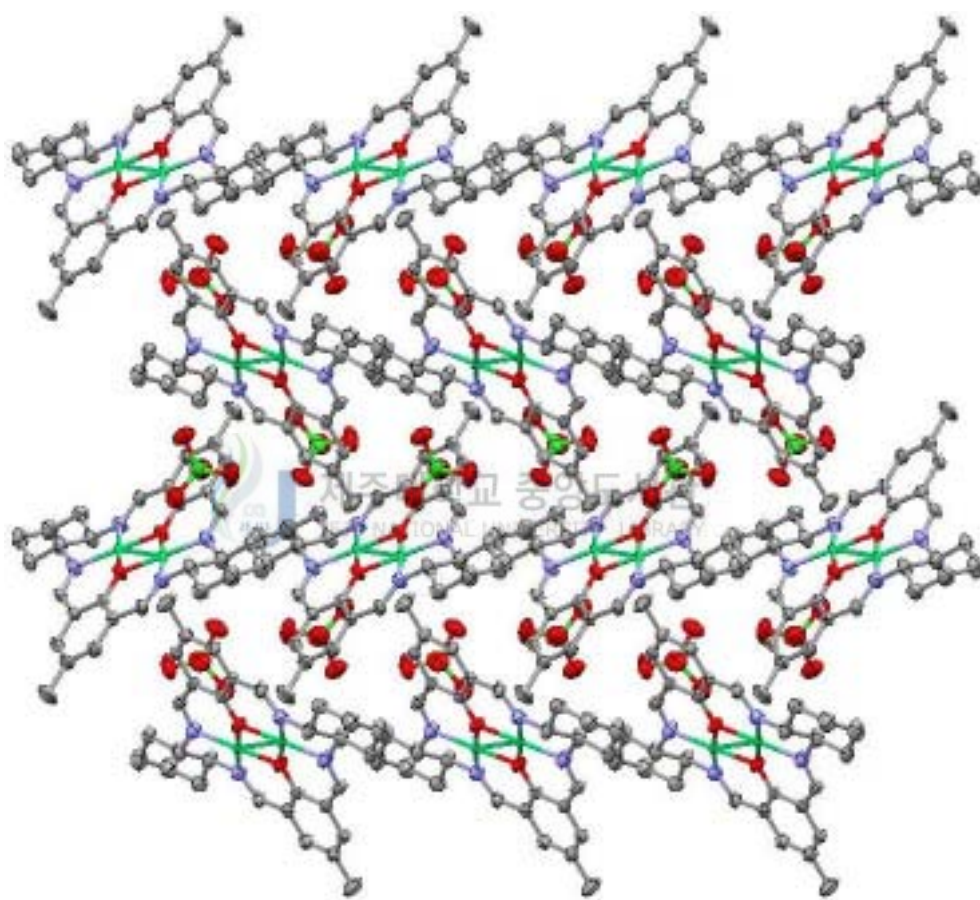


Figure 30. The molecular packing diagram of $[\text{Ni}(\text{H}_2[20]\text{-DCHDC})](\text{ClO}_4)_2$.

Table 15. Bond lengths (Å) for [Ni(H₂[20]-DCHDC)](ClO₄)₂ complex

Ni(1)-O(1)#1	1.743(4)	C(1)-C(2)	1.416(8)
Ni(1)-O(1)	1.816(4)	C(2)-C(3)	1.402(8)
Ni(1)-N(2)	1.865(5)	C(2)-C(14)#1	1.448(8)
Ni(1)-N(1)	1.907(6)	C(3)-C(4)	1.365(9)
Ni(1)-Ni(1)#1	2.617(2)	C(4)-C(5)	1.382(9)
Cl(1)-O(3)	1.409(5)	C(4)-C(15)	1.511(9)
Cl(1)-O(4)	1.442(6)	C(5)-C(6)	1.412(9)
Cl(1)-O(5)	1.444(6)	C(6)-C(7)	1.442(8)
Cl(1)-O(2)	1.450(6)	C(8)-C(9)	1.516(9)
O(1)-C(1)	1.323(7)	C(8)-C(13)	1.524(9)
O(1)-Ni(1)#1	1.743(4)	C(9)-C(10)	1.534(9)
N(1)-C(7)	1.295(8)	C(10)-C(11)	1.462(10)
N(1)-C(8)	1.500(8)	C(11)-C(12)	1.525(9)
N(2)-C(14)	1.294(8)	C(12)-C(13)	1.522(9)
N(2)-C(13)	1.489(8)	C(14)-C(2)#1	1.448(8)
C(1)-C(6)	1.394(8)		

Symmetry transformations used to generate equivalent atoms:

#1 -x+1, y, z.

Table 16. Angles [°] for [Ni(H₂[20]-DCHDC)](ClO₄)₂ complex

O(1)#1-Ni(1)-O(1)	85.37(19)	O(1)-C(1)-C(2)	120.0(5)
O(1)#1-Ni(1)-N(2)	94.9(2)	C(6)-C(1)-C(2)	119.1(5)
O(1)-Ni(1)-N(2)	178.8(2)	C(3)-C(2)-C(1)	118.8(6)
O(1)#1-Ni(1)-N(1)	176.5(2)	C(3)-C(2)-C(14)#1	118.8(5)
O(1)-Ni(1)-N(1)	91.7(2)	C(1)-C(2)-C(14)#1	122.3(5)
N(2)-Ni(1)-N(1)	88.0(2)	C(4)-C(3)-C(2)	122.4(6)
O(1)#1-Ni(1)-Ni(1)#1	43.76(13)	C(3)-C(4)-C(5)	118.9(6)
O(1)-Ni(1)-Ni(1)#1	41.61(14)	C(3)-C(4)-C(15)	121.5(6)
N(2)-Ni(1)-Ni(1)#1	138.68(18)	C(5)-C(4)-C(15)	119.6(6)
N(1)-Ni(1)-Ni(1)#1	133.27(17)	C(4)-C(5)-C(6)	121.1(6)
O(3)-Cl(1)-O(4)	109.7(4)	C(1)-C(6)-C(5)	119.7(5)
O(3)-Cl(1)-O(5)	111.2(4)	C(1)-C(6)-C(7)	122.7(5)
O(4)-Cl(1)-O(5)	108.2(4)	C(5)-C(6)-C(7)	117.7(6)
O(3)-Cl(1)-O(2)	110.1(4)	N(1)-C(7)-C(6)	124.5(6)
O(4)-Cl(1)-O(2)	109.0(4)	N(1)-C(8)-C(9)	114.8(5)
O(5)-Cl(1)-O(2)	108.6(3)	N(1)-C(8)-C(13)	105.7(5)
C(1)-O(1)-Ni(1)#1	130.6(4)	C(9)-C(8)-C(13)	111.5(6)
C(1)-O(1)-Ni(1)	130.2(4)	C(8)-C(9)-C(10)	109.6(6)
Ni(1)#1-O(1)-Ni(1)	94.63(19)	C(11)-C(10)-C(9)	111.8(6)
C(7)-N(1)-C(8)	125.4(5)	C(10)-C(11)-C(12)	114.4(6)
C(7)-N(1)-Ni(1)	125.1(4)	C(13)-C(12)-C(11)	109.1(6)
C(8)-N(1)-Ni(1)	109.0(4)	N(2)-C(13)-C(12)	116.2(6)
C(14)-N(2)-C(13)	125.9(5)	N(2)-C(13)-C(8)	105.3(5)
C(14)-N(2)-Ni(1)	123.8(4)	C(12)-C(13)-C(8)	110.3(6)
C(13)-N(2)-Ni(1)	110.1(4)	N(2)-C(14)-C(2)#1	124.3(5)
O(1)-C(1)-C(6)	120.9(5)		

Symmetry transformations used to generate equivalent atoms:

#1 -x+1, y, z.

IV. Conclusion

Binuclear Ni(II) complex $\{[\text{Ni}_2([\text{20}]\text{-DCHDC})]\text{Cl}_2\}$, with $[2 + 2]$ symmetrical N_4O_2 compartmental macrocyclic ligand $\{\text{H}_2[\text{20}]\text{-DCHDC}$; 14,29-dimethyl-3,10,18,25-tetraazapentacyclo-[25,3,1,0^{4,9},1^{12,16},0^{19,24}]ditriacontane-2,10,12,14,16(32),17,27(31),28,30-decane-31,32-diol} containing bridging phenolic oxygen atoms was synthesized by metal template condensation of 2,6-diformyl-*p*-cresol, *trans*-1,2-diaminocyclohexane and nickel chloride hexahydrate. The reaction of $[\text{Ni}_2([\text{20}]\text{-DCHDC})]\text{Cl}_2$ with auxiliary ligands (L_a ; ClO_4^- , SCN^- , N_3^- , NO_2^- and Γ) in methanol solution formed a new 5 complexes; $[\text{Ni}_2([\text{20}]\text{-DCHDC})](\text{ClO}_4)_2$, $[\text{Ni}_2([\text{20}]\text{-DCHDC})(\text{NCS})_2]$, $[\text{Ni}_2([\text{20}]\text{-DCHDC})(\text{N}_3)_2]$, $[\text{Ni}_2([\text{20}]\text{-DCHDC})-(\mu\text{-ONO})\text{NO}_2 \cdot 1.5\text{H}_2\text{O}$, and $[\text{Ni}_2([\text{20}]\text{-DCHDC})\text{I}_2]$. Mononuclear Ni(II) complex $([\text{Ni}(\text{H}_2[\text{20}]\text{-DCHDC})](\text{ClO}_4)_2 \cdot 2\text{H}_2\text{O})$, with $[2+2]$ symmetrical N_4O_2 compartmental macrocyclic ligand containing bridging phenolic oxygen atoms was synthesized by metal template condensation of 2,6-diformyl-*p*-cresol, *trans*-1,2-diaminocyclohexane and nickel perchlorate hexahydrate. The reaction of $[\text{Ni}(\text{H}_2[\text{20}]\text{-DCHDC})](\text{ClO}_4)_2 \cdot 2\text{H}_2\text{O}$ with auxiliary ligand (L_a ; SCN^-) in methanol solution formed $[\text{Ni}(\text{H}_2[\text{22}]\text{-DCHDC})(\text{NCS})_2] \cdot 3\text{H}_2\text{O}$.

X-ray crystals and molecular structures of $[\text{Ni}_2([\text{20}]\text{-DCHDC})](\text{ClO}_4)_2 \cdot 2\text{CH}_3\text{CN}$ have been determined on a X-ray diffractometer. In $[\text{Ni}_2([\text{20}]\text{-DCHDC})](\text{ClO}_4)_2$ complex, a total 3837 reflections at the $2\sigma(I)$ significance were used to give final discrepancy indices of $R_1 = 0.0580$ and $wR_2 = 0.1507$. The complex crystallizes in the monoclinic space group $P_2(1)c$ in a cell having the dimensions $a = 9.2745(5)$ Å, $b = 18.9687(10)$ Å, and $c = 11.0198(6)$ Å. The calculated density is $1.556\text{g}/\text{cm}^3$. Two formula units comprise the unit cell with half of the binuclear complex in the asymmetric unit. The binuclear core structures are centrosymmetric with each nickel(II)

ion in the N_2O_2 sites being four-coordinate by square-planar geometry of interactions with two nitrogen and two oxygen atoms of the binucleating ligand [20]-DCHDC. $[Ni_2([20]-DCHDC)](ClO_4)_2 \cdot 2CH_3CN$ has two uncoordinated perchlorate anions, two acetonitrile molecule in the crystal lattice. The Ni-N(3) (acetonitrile) separation is 3.256 Å. The Ni-O(16) (perchlorate) separation is 4.759 Å, The interatomic Ni \cdots Ni separation is 2.8078(10) Å. The in-plane Ni-to-donor distances range from 1.827(3) to 1.842(3). The macrocyclic complex adopts an essentially flat structure with the two square-plane nickel centers bridged by the two phenoxide oxygen atoms; the dihedral angle between the plane defined by N(1), O(1), and O(1)# and the plane defined by Ni(1)#, O(1), and O(1)# is 178.01°. The sum of angles at the nickel basal planes (NiN₂O₂) is almost exactly 360° (359.79°), indicating no plane distortion. The angle of C(1)-O(1)-O(1)# is 166.55°. This value is smaller than the ideal value of 180°, indicating that the two phenol mean planes are not able to flat.

X-ray crystals and molecular structures of $[Ni(H_2[20]-DCHDC)](ClO_4)_2$ have been determined on a Bruker SMART diffractometer. In $[Ni(H_2[20]-DCHDC)](ClO_4)_2$ complex, a total 3205 reflections at the $2\sigma(I)$ significance were used to give final discrepancy indices of $R_1 = 0.0811$ and $wR_2 = 0.1984$. The complex crystallizes in the monoclinic space group $P_2(1)c$ in a cell having the dimensions $a = 9.2033(5)$ Å, $b = 14.6208(8)$ Å, and $c = 11.8316(7)$ Å. The calculated density is 1.572 g/cm³. Two formula units comprise the unit cell with half of the mononuclear complex in the asymmetric unit. The occupancy of central metal Ni(II) is 0.5. The geometry about Ni(1) in the N_2O_2 site is a square-planar environment, and other N_2O_2 site is able to vacant. The macrocyclic complex adopts an essentially flat structure with the square-planar nickel center bridged by the two phenoxide oxygen atoms the dihedral angle between the plane defined by N(1A), O(1), and O(1A) and the

plane defined by Ni(1), O(1), and O(1A) is 179.15°. The sum of angles at the nickel basal planes (NiN₂O₂) is almost exactly 360° (359.97°), indicating no plane distortion. The angle of C(1)-O(1)-O(1A) is 162.80°. This value is smaller than the ideal value of 180°, indicating that the two phenol mean planes are not able to flat. The in-plane Ni-to-donor distances range from 1.743(4) to 1.907(6) Å. The perchlorate ions occupy lattice sites. The Ni(1)···O(2) (perchlorate) separation is 3.453(6) Å. A strong ionic ClO₄⁻ band at near 1107 cm⁻¹ and 622 cm⁻¹ in [Ni₂([20]-DCHDC)](ClO₄)₂ complex. The absorption vibrations due to the N-coordinated bonded NCS⁻ in [Ni₂([20]-DCHDC)(NCS)₂] appear 2044 and 871 cm⁻¹. The absorption peak at 2015 cm⁻¹ in the [Ni₂([20]-DCHDC)(N₃)₂] is assigned to the asymmetric stretching mode of coordinated azide. The symmetric stretching frequency of coordinated azide is observed at 1346 cm⁻¹. The strong absorption peaks at 1450 and 1238 cm⁻¹ in the [Ni₂([20]-DCHDC)(μ-ONO)]NO₂ · 1.5H₂O are assigned to a bridging bidentate ligand Ni-ONO-Ni. And stretching bands of NO₂ counter ion are observed at 1327 and 1272 cm⁻¹. A strong ionic ClO₄⁻ band at near 1089 cm⁻¹ and 622 cm⁻¹ in [Ni(H₂[20]-DCHDC)](ClO₄)₂·2H₂O complex. The absorption vibrations due to the N-coordinated bonded NCS⁻ and ionic NCS⁻ groups in [Ni(H₂[20]-DCHDC)(NCS)₂] · 3H₂O appear 2044 and 869 cm⁻¹. The [Ni₂([20]-DCHDC)]⁺ species of these complexes are well observed in the FAB mass spectra at m/z 598 region. α-Cleavage peaks of one cyclohexane from the [Ni₂([20]-DCHDC)]⁺ ion in the formation of the fragment [Ni₂(L_{ac})]⁺ are observed at m/z 516 region. Removal peaks of one nickel ion from the [Ni₂([20]-DCHDC)]⁺ ion in the formation of the fragment [Ni([20]-DCHDC)]⁺ is observed at m/z 541. The FAB mass spectra of all the complexes contain peaks corresponding to the [H₂[20]-DCHDC]⁺ fragment ion at m/z 484 region. This indicates that the species [Ni₂([20]-DCHDC)]⁺ undergoes demetallation to give the tetraazadioxa macrocycle H₂[20]-DCHDC

under FAB conditions. These peaks are associated with peaks of mass one or two greater or less, which are attributed to protonated/deprotonated forms.



References

- [1] B. Dietrich, P. Viout, and J. -M. Lehn, *Macrocyclic Chemistry*, VCH Verlagsgesellschaft, Weinheim, **1993**.
- [2] J. M. Lehn, *Supramolecular Chemistry*, VCH Verlagsgesellschaft, Weinheim, **1995**.
- [3] E. C. Constable, *Metals and Ligand Reactivity*, VCH Verlagsgesellschaft, Weinheim, **1996**.
- [4] J. R. Fredericks and A. D. Hamilton, in: A. D. Hamilton (Ed.), *Supramolecular Control of Structure and Reactivity*, Wiley, Chichester, **1996**, Chapter 1.
- [5] J. W. Steed and J. L. Atwood, *Supramolecular Chemistry*, Wiley, Chichester, **2000**.
- [6] E. Kimura, I. Nakamura, T. Koike, M. Shionoya, Y. Kodama, T. Ikeda, and M. Shiro, *J. Am. Chem. Soc.* **1994**, 116, 4764
- [7] J. H. Kim, *Chem. Lett.* **2000**, 156.
- [8] E. L. Hegg, S. H. Mortimore, C. L. Cheung, J. E. Huyett, D. R. Powell, and J. N. Burstyn, *Inorg. Chem.* **1999**, 38, 2961.
- [9] K. A. Deal, A. C. Hengge, and J. N. Burstyn, *J. Am. Chem. Soc.* **1996**, 118, 1713.
- [10] K. A. Deal and J. N. Burstyn, *Inorg. Chem.* **1996**, 35, 2792.
- [11] W. H. Jr. Chapman, and R. Breslow, *J. Am. Chem. Soc.* **1995**, 117, 5462.
- [12] P. Rossi, F. Felluga, P. Tecilla, F. Formaggio, M. Crisma, C. Toniolo, and P. Scrimin, *J. Am. Chem. Soc.* **1999**, 121, 6948.
- [13] E. L. Hegg, K. A. Deal, L. L. Kiessling, and J. N. Burstyn, *Inorg. Chem.* **1997**, 36, 1715.

- [14] C. Sissi, P. Rossi, F. Felluga, F. Formaggio, M. Palumbo, P. Tecilla, C. Toniolo, P. Scrimin, *J. Am. Chem. Soc.* **2001**, 123, 6948.
- [15] E. L. Hegg and J. N. Burstyn, *Inorg. Chem.* **1996**, 35, 7474.
- [16] E. L. Hegg and J. N. Burstyn, *J. Am. Chem. Soc.* **1995**, 117, 7015.
- [17] F. Liang, C. Wu, H. Lin, T. Li, D. Gao, Z. Li, J. Wei, C. Zheng, M. Sun, *Bioorg. Med. Chem. Lett.* **2003**, 13, 2469.
- [18] F. Liang, P. Wang, X. Zhou, T. Li, Z. Li, H. Lin, D. Gao, C. Zheng, and C. Wu, *Bioorg. Med. Chem. Lett.* **2004**, 14, 1901.
- [19] D. Kong, J. Mao, Arthur E. Martell *Inorg. Chim. Acta* **2002**, 335, 7.
- [20] O. Kahn, *Structure and Bonding(Berlin)* **1987**, 68, 89.
- [21] T. Shozo, *Bull. Chem. Soc. Jpn.* **1984**, 57, 2683.
- [22] J. C. Byun, Y. C. Park, and C. H. Han, *J. Kor. Chem. Soc.* **1999**, 43/3, 267.
- [23] Bruker, *SAINTPLUS NT Version 5.0. Software Reference Manual Bruker AXS: Madison, Wisconsin*, **1998**.
- [24] L. A. Kahwa, J. Selbin, T. C. Y. Hsieh and R. A. Laine, *Inorg. Chim. Acta* **1986**, 118, 179.
- [25] D. Suresh Kumar and V. Alexander, *Inorg. Chim. Acta* **1995**, 238, 63.
- [26] G. Socrates, *Infrared and Raman Characteristic Group Frequencies*. 3rd edn., Wiley, New York, **2001**, p. 299.
- [27] G. Socrates, *Infrared and Raman Characteristic Group Frequencies*. 3rd edn., Wiley, New York, **2001**, p. 320.
- [28] G. Socrates, *Infrared and Raman Characteristic Group Frequencies*. 3rd edn., Wiley, New York, **2001**, p. 321.
- [29] G. Socrates, *Infrared and Raman Characteristic Group Frequencies*. 3rd edn., Wiley, New York, **2001**, p. 317.
- [30] D. Sutton, *Electronic Spectra of Transition Metal Complexes*, McGraw-Hill, London, **1968**.

국 문 초 록

2,6-diformyl-*p*-cresol과 *trans*-1,2-diaminocyclohexane을 $\text{NiCl}_2 \cdot 6\text{H}_2\text{O}$ 를 이용한 금속주형 축합반응을 통해 페놀의 산소원자가 다리 결합을 하고 있는 이핵 Ni(II)의 20-원 페놀 바탕 N_4O_2 칸막이형 거대고리 $\{\text{H}_2[20]\text{-DCHDC}; 14,29\text{-dimethyl-}3,10,18,25\text{-tetraazapentacyclo-}[25,3,1,0^{4,9},1^{12,16},0^{19,24}]\text{ditriacontane-}2,10,12,14,16(32),17,27(31),28,30\text{-decane-}31,32\text{-diol}\}$ $[\text{Ni}_2([20]\text{-DCHDC})]\text{Cl}_2$ 착물이 합성 하였다. $[\text{Ni}_2([20]\text{-DCHDC})]\text{Cl}_2$ 을 메탄을 용매 하에서 보조리간드(L_a) (L_a ; ClO_4^- , SCN^- , NO_2^- , N_3^- , I^-)와 반응시켜 새로운 이핵 Ni(II) 착물 5개, $[\text{Ni}_2([20]\text{-DCHDC})](\text{ClO}_4)_2$, $[\text{Ni}_2([20]\text{-DCHDC})(\text{NCS})_2]$, $[\text{Ni}_2([20]\text{-DCHDC})(\text{N}_3)_2]$, $[\text{Ni}_2([20]\text{-DCHDC})(\mu\text{-ONO})]\text{NO}_2 \cdot 1.5\text{H}_2\text{O}$, $[\text{Ni}_2([20]\text{-DCHDC})\text{I}_2]$ 가 합성 되었다. 그러나 2,6-diformyl-*p*-cresol과 *trans*-1,2-diaminocyclohexane을 $\text{Ni}(\text{ClO}_4)_2$ 를 이용한 금속주형 축합반응을 시킬 경우 페놀의 산소원자가 다리 결합을 하고 있는 단핵 Ni(II)의 20-원 페놀 바탕 N_4O_2 칸막이형 거대고리 $[\text{Ni}(\text{H}_2[20]\text{-DCHDC})](\text{ClO}_4)_2 \cdot 2\text{H}_2\text{O}$ 착물이 합성 되었다. 이 착물을 메탄을 용매 하에서 SCN^- 를 반응시켜 새로운 단핵 Ni(II) 착물, $[\text{Ni}([22]\text{-DCHDC})(\text{NCS})_2] \cdot 3\text{H}_2\text{O}$ 이 합성 하였다.

이 착물 중 $[\text{Ni}_2([20]\text{-DCHDC})](\text{ClO}_4)_2 \cdot 2\text{CH}_3\text{CN}$, $[\text{Ni}(\text{H}_2[20]\text{-DCHDC})](\text{ClO}_4)_2$ 결정구조 분석하였다. $[\text{Ni}_2([20]\text{-DCHDC})](\text{ClO}_4)_2 \cdot 2\text{CH}_3\text{CN}$ 착물은 거대고리 내에 N_2O_2 자리에 각각 Ni(II)금속이 네자리 배위수를 갖는 사각평면구조를 이루고 있다. 결정격자에 존재하는 CH_3CN 분자는 중심금속으로부터 3.256 Å 떨어져 있고, perchlorate 이온은 4.759 Å 떨어져 있다. Ni...Ni 간은 2.8078(10) Å 떨어져 있다 $[\text{Ni}(\text{H}_2[20]\text{-DCHDC})](\text{ClO}_4)_2$ 착물은 거대고리 내에 N_2O_2 자리에 0.5 개의 Ni(II)금속이 존재하며 금속과 결합되어 있는 N_2O_2 자리는 사각평면구조를 이루고 있다. Ni(II)금속과 주개 원자 간의 거리는 1.743(4) 에서 1.907(6) Å이고, 결정격자내의 ClO_4^- 이온은 Ni(II)금속과 3.453(6) Å 떨어져 있다.

감 사 의 글

저 이제 졸업 합니다...^^

짧은 대학원 시간을 돌이켜 보며 감사해야 할 분들에게 아무런 말없이 떠나게 되는 것 같아 이렇게 짧게나마 감사드리고 싶습니다.

우선 학부 때부터 지금까지 부족한 제게 많은 조언과 관심으로 이끌어 주셨던 변종철 교수님께 진심으로 감사드리고 지금에 이르기까지 늘 격려 해주시고 용기를 북돋워 주신 한성빈 교수님, 정덕상 교수님, 김덕수 교수님, 강창희 교수님, 이선주 교수님, 김원형 교수님 이남호 교수님께 진심으로 감사를 드립니다.

그리고 친형처럼, 무서운 선생님이로 늘 채찍질 해주신 한충훈 선생님, 우리형수님과 늘 격려해주신 무기화학실험실에 문대훈, 이우환, 김구철 선생님께 감사드리고, 우리 실험실에 말 안 듣는 보철이, 이뿐이 한나, 착한 동호, 남친 생긴 송정이, 선배가 그리 잘한 건 없지만 늘 따라주고 웃는 모습 보여줘서 고맙다. 그리고 학부 때부터 같이한 우리 친구들, 화학과 선후배들에게 감사드리고, 나 없이 무슨 재미로 학교생활 할지 심히 걱정이 됩니다.

마지막으로 힘들게 생활하시면서 못난 아들 믿고 지금까지 지켜봐 주신 사랑하는 아버지, 어머니, 그리고 두 누님과 사랑하는 여동생에게 진심으로 감사합니다.

여러분 모두를 사랑합니다...^^